

REHABILITATION OF DAMAGED CONCRETE USING ECO-FRIENDLY BACILLUS SUSPENDED GROUT



Final Year Project UG 2016

By

Maaz Khalid

Affan Ul Haq

Farhad Ahmad

Aman Ullah

Supervisor

Asst. Prof. Dr. Rao Arsalan Khushnood

NUST Institute of Civil Engineering
School of Civil and Environmental Engineering
National University of Sciences and Technology, Islamabad
Pakistan
2020

Rehabilitation of Damaged Concrete using Eco-Friendly Bacillus Suspended Grout



Final Year Project UG 2016

By

Maaz Khalid	00000 173402
Affan Ul Haq	00000 174358
Farhad Ahmad	00000 127542
Aman Ullah	00000 129549

NUST Institute of Civil Engineering
School of Civil and Environmental Engineering
National University of Sciences and Technology, Islamabad
Pakistan
2020

This is to certify that the
Final Year Project Titled
**“Rehabilitation of Damaged Concrete using Eco-Friendly
Bacillus Suspended Grout”**

Submitted By

Maaz Khalid	00000 173402
Affan Ul Haq	00000 174358
Farhad Ahmad	00000 127542
Aman Ullah	00000 129549

has been accepted towards the requirements
for the undergraduate degree

in

CIVIL ENGINEERING

Dr. Rao Arsalan Khushnood
Head of Structural Engineering
Department NUST Institute of Civil
Engineering

School of Civil and Environmental Engineering
National University of Sciences and Technology, Islamabad

ACKNOWLEDGEMENTS

In the name of Allah, the most Beneficent, the most Merciful as well as peace and blessings upon Prophet Muhammad, His servant and final messenger.

We are first and foremost, extremely grateful to Allah Almighty for enabling us to complete our research project and without Whose willingness we could not have imagined to accomplish such an enormous task.

The efforts and sacrifices that our parents and teachers have made over the course of our lives to reach where we stand today are highly acknowledged. Special mention of our siblings who were a source of constant motivation and stood by our sides during tough times.

We respect and appreciate the efforts put up by our supervisor Dr. Rao Arsalan Khushnood, Head of Structural Engineering Department. His valuable advice and research commitments were a source of motivation for us. Throughout the research project his constant support and taking time out of his busy schedule for mentorship kept us proceeding forward. Moreover, his professional grooming of the group in thesis writing and presentation is valuable and something that will help us in our practical life.

We would express our gratitude towards Dr. Zeeshan Ali Khan, IESE, NUST providing expertise in development of climate control chamber and permitting us to use the pyrolysis setup. We are thankful to the lab staff of mentioned departments for their assistance in performing the lab tests.

We are extremely grateful to Ms. Nafeesa Shaheen, PG student at NICE, for providing us bacterial culture as well as guiding us throughout the research and practical phase of the project. We are thankful to Mr. Asim sultan and Mr. Ateeb Muhammad Ali, PG student at NICE for helping us in execution of some tests. We value the assistance provided by the entire staff (Mr Riasat, Faheem, and Ismail) of Structures Lab, NICE. Special thanks to Lab Engr. Mati Ullah Shah and Atif Mehmood in coordinating for our testing.

Finally, we would extend our appreciation towards our friends and colleagues who kept encouraging us and provided necessary assistance in completion of this research project.

Dedication

To

*Our Advisor Dr. Rao Arsalan Khushnood
& Our Families*

ABSTRACT

Construction pattern in Pakistan throughout the decades has expanded suddenly which calls for expanded construction to meet the demands of ever-growing population. Construction sector is one of the significant contributors of CO₂ emissions that has led to world facing green-house gases, global warming, and health issues. Since concrete is a popular construction material principally due to its strength, it has the tendency to develop micro structural cracks because of low tensile strength, that gradually deteriorates its properties owing to embedded reinforcement exposed to chloride ions that leads to corrosion. Various commercially available techniques are currently a potential remedy to this problem. Numerous researches have been conducted to investigate the performance of these commercial techniques and it has been concluded that these are expensive and have failed to provide a long-term solution. A bacillus suspended grout can be a solution to rehabilitate concrete. Various researches have been conducted to investigate self-healing concrete and bio-influenced self-healing has been concluded to be the best approach in terms of crack healing and strength recovery. Same technique can be used to prepare a grout that ensures long term crack repair, whose performance will depend on using an effective micro/nano immobilizer. In this research study, 5 different formulations were made using nano/micro zeolite and Super Absorbent Polymer (SAP) as immobilizer and were used to examine crack repairing at various ages, quantifying CO₂ sequestration ability, investigating the corrosion potential and analyzing autonomous healing at various cracking cycle. Optical Microscopy, X-ray Diffraction (XRD), Thermogravimetric Analysis (TGA), Strength Recovery Index (SRI) and Ultrasonic Pulse Velocity (UPV) were conducted to verify crack repair. CO₂ sequestration ability was quantified by developing a climate control chamber and modelling a room. Corrosion was examined through Weight Loss Measurement. Visual evidence was obtained to analyze autonomous healing at various cracking cycles. Experimental results reveal that zeolite and SAP both are an effective carrier to immobilize bacteria, but the Bacterial Zeolite (BZ) grout gave the optimum results by recovering compressive and tensile strength up to 96.73% and 92.51% respectively, CO₂ sequestration ability of bacterial zeolite grout is 32 times that of non-bacterial grout, corrosion potential was found to be only 1.13% loss in rebar weight and maximum autonomous healing was reported to be 3.3 mm for the second cracking cycle.

TABLE OF CONTENTS

LIST OF FIGURES	vi
LIST OF TABLES	viii
LIST OF ACRONYMS	ix
CHAPTER 1	
INTRODUCTION	1
1.1 General.....	1
1.2 Rehabilitation of Concrete	1
1.3 Self-Healing Concrete.....	1
1.4 Environmental Impact	2
1.5 Problem Statement	2
1.6 Objectives	3
1.7 Thesis Structure.....	3
CHAPTER 2	
LITERATURE REVIEW	4
2.1 Self-Healing	4
2.1.1 Characteristics of Repaired Dead Concrete.....	4
2.1.2 Characteristics of Self-Healing Behaviour.....	5
2.1.3 Classification based on Self-Healing Behaviour.....	6
2.1.4 Non-Biological Techniques of Self-Healing.....	6
2.1.5 Bio-Influenced Self-Healing.....	6

2.1.6 Biological Process of Microbial Induced Calcite Precipitation.....	6
2.1.7 Bacterial Concentration.....	7
2.1.8 Carrier Materials	8
2.1.9 Influence of Nutrients.....	8
2.1.10 Improvements in Characteristics.....	8
2.1.11 Water – Cement Ratio.....	9
2.2 Corrosion.....	9
2.2.1 Introduction.....	9
2.2.2 Corrosion Process.....	10
2.2.3 Corrosion Rate.....	10
2.2.4 Carbonation-Induced Corrosion.....	12
CHAPTER 3	
MATERIALS AND EXPERIMENTAL METHODOLOGY	13
3.1 Materials.....	13
3.1.1 Zeolite	13
3.1.2 SAP	14
3.1.3 Bacteria	14
3.1.4 Calcium Lactate.....	15
3.1.5 Cement	16
3.1.6 Sand.....	16
3.1.7 Aggregate.....	17
3.1.8 Steel.....	17
3.2 Experimental Methodology.....	17

3.2.1 Mix Design.....	18
3.2.2 Mixing Regime.....	19
3.2.3 Curing.....	20
3.2.4 Application.....	20
CHAPTER 4	
EXPERIMENTAL TEST AND RESULTS	22
4.1 Healing Analysis.....	22
4.1.1 Crack Width Measurements Analysis.....	22
4.1.2 Thermogravimetric Analysis.....	23
4.1.3 X-Ray Diffraction Analysis.....	24
4.1.4 Strength Recovery Index.....	26
4.1.5 Ultraviolet Pulse Velocity.....	32
4.2 Corrosion.....	35
4.2.1 Weight Loss Measurement.....	35
4.3 CO ₂ Monitoring	37
4.3.1 Climate Controlled Chamber	37
4.3.2 Room Model.....	40
4.4 Healing Cycles.....	41
4.4.1 Visual Evidence	41
4.5 Cost Estimation	42

CHAPTER 5

CONCLUSIONS.....	43
RECOMMENDATIONS.....	44
CONSTRAINTS.....	45
REFERENCES.....	46

LIST OF FIGURES

Figure 1: Free shrinkage of PCC with time	4
Figure 2: Free shrinkage of SIKA Repair Mortar with time.....	5
Figure 3: Free shrinkage of BSAF Nanocrete with time	5
Figure 4: Stages of crack healing in concrete	7
Figure 5: Stages in corrosion induced damage	9
Figure 6: Schematics of corrosion process	10
Figure 7: Relationship between Cl ⁻ concentration and pH.....	11
Figure 8: Relationship between corrosion penetration depth and service life of structure	12
Figure 9: Particle size analysis of Zeolite	13
Figure 10: Particle size analysis of SAP	13
Figure 11: Prepared solution of bacillus subtilis	15
Figure 12: Particle size distribution of sand.....	16
Figure 13: Pictorial representation of Application	21
Figure 14: OM image of BS	22
Figure 15: TGA of BG and BS	23
Figure 16: XRD of BS	24
Figure 17: XRD of BG.....	24
Figure 18: XRD of BZ	25
Figure 19: XRD of BSAP	25
Figure 20: Compounds identified using XRD	25
Figure 21: Compressive strengths at (a) 3 days (b) 7 days (c) 14 days (d) 28 days of cured sample	28

Figure 22: Compressive strength recovery rate with healing age	28
Figure 23: Compressive Strength recovery matrix for different formulations	29
Figure 24: Tensile strengths at (a) 3 days (b) 7 days (c) 14 days (d) 28 days of cured sample	31
Figure 25: Tensile strength recovery rate with healing age	31
Figure 26: Tensile Strength recovery matrix for different formulations.....	32
Figure 27: UPV on (a) 3 days (b) 7 days (c) 14 days (c) 28 days, uncracked, cracked and healed samples	34
Figure 28: UPV recovery rate with healing age	35
Figure 29: Pictorial description of weight loss measurement test.....	36
Figure 30: Weight loss measurement results	36
Figure 31: Schematics of climate control chamber.....	37
Figure 32: Real time CO ₂ monitoring in the climate control chamber	37
Figure 33: CO ₂ monitoring result extracted from sensor.....	38
Figure 34: CO ₂ monitoring result of BZ extracted from sensor.....	39
Figure 35: Phenolphthalein test for NBG.....	39
Figure 36: Phenolphthalein test for BZ	40
Figure 37: Hypothetical room model (a) elevation (b) plan (c) front view	40
Figure 38: Autonomous healing of BZ repaired sample in 2 nd Cracking cycle.....	41
Figure 39: OM image of 2nd healing cycle of BZ repaired concrete	42

LIST OF TABLES

Table 1: Compound in Zeolite.....	13
Table 2: Properties of SAP.....	14
Table 3: Properties of calcium lactate.....	15
Table 4: Properties of cement.....	16
Table 5: Properties of sand.....	17
Table 6: Properties of aggregates.....	17
Table 7: Properties of steel.....	17
Table 8: Details of casting.....	18
Table 9: Details of concrete mix design.....	18
Table 10: Details of formulations of grouts.....	19
Table 11: Procedure for concrete preparation.....	19
Table 12: Procedure for grouts preparation.....	20
Table 13: Summary of CWMA results.....	22
Table 14: Summary of room model calculations.....	41
Table 15: Cost estimation of BZ.....	42
Table 16: Cost estimation of epoxy grout.....	42

LIST OF ACRONYMS

ASTM	American Society of Testing and Materials
CWMA	Crack Width Measurement Analysis
f_c'	Compressive Strength
LWA	Light Weight Aggregates
OM	Optical Microscopy
SRI	Strength Recovery Index
TGA	Thermogravimetric Analysis
UPV	Ultrasonic Pulse Velocity
UTM	Universal Testing Machine
XRD	X-Ray Diffraction
NBG	Non-Bacterial Grout
BS	Bacterial Spray
BG	Bacterial Grout
BZ	Zeolite immobilized Bacterial Grout
BSAP	SAP immobilized Bacterial Grout

INTRODUCTION

1.1 General

Concrete is the second most consumed material after water in the world. Concrete being a composite material has been widely availed in construction sector due to its mechanical strength, durability, impact resistance and insulation properties. Globally an escalation was noted in the demand for concrete in year 1950 and it reached the maximal in year 2000 after which a persistent trend has been noted. However, concrete being a brittle material and incorporating low tensile strength, an exponential rise has been recorded in structures needing rehabilitation since year 1980. It is estimated that annual repair cost of concrete in US is \$18-21 billion. Furthermore, the structures also require recurrent maintenance that accounts for a notable cost. Therefore, it is essential to create an effective repairing technique that can fulfill the growing need of repairing structures.

1.2 Rehabilitation of Concrete

Structures that experience settlements and force majeure like earthquake, flood etc. are agonized by cracks. It has been noted that these cracks can be repaired in a cost that is a just a minor part of the cost of new structure. Repairing a structure also saves a considerable time rather than reconstructing it. Rehabilitation of a structure is essential for its stability and aesthetics. The factors that govern the performance of repairing techniques are performance, cost, simplicity, speed of application and availability. Various techniques are commercially being used to repair concrete like grouting, epoxy injection, stitching etc. However, all of them have the constraints of performance and cost.

1.3 Self-Healing Concrete

Self-healing concrete is an autonomously crack repairing concrete that contains bacterial species to ensure repairing. When a crack propagates in this concrete due to moisture seepage the dormant bacterial spores become active through metabolism thus repairing cracks through calcite precipitation and reducing further ingress of water into cracks. Bacteria in isolation cannot survive in concrete due to high mechanical stresses and high pH environment, it needs to be introduced using an immobilizer of micro/nano particles. It is an eco-friendly and natural driven technique.

1.4 Environmental Impact

Construction sector consumes large amount of unrenovable energy and causing large emissions of carbon dioxide. Building and construction are responsible for 39% of all carbon dioxide emission in the world with production and logistics of cement being the main factors. However, the process of calcite precipitation in self-healing consumes carbon dioxide that lowers the amount of carbon emission in atmosphere.

1.5 Problem Statement

In the past, various techniques have been used to repair cracks in concrete like grouting, epoxy injection etc. However, in case of grouting the differential shrinkage between new overlay grout and that of old underlying concrete triggers shrinkage stresses that are tensile in nature and resulting in cracking when this tensile stress reaches the tension capacity of overlay grout. Moreover, epoxy injection requires a large amount of energy for production, is also very expensive and cracks can reform in it.

Numerous products have been introduced in market that once repairs the crack constructively and partially or completely regains the strength of underlying substrate concrete, but no product has been introduced that repairs the crack effectively once but also re-repairs the old substrate concrete if cracked again.

Self-healing concrete have been proven effective through various researches which shows that when crack propagates in it and water seeps into the crack, it precipitates calcite through bacterial metabolism and repairing the crack. However, no research has been carried out till date to introduce a product that repairs normal concrete (no tendency of self-healing) using the mechanism of self-healing concrete. Doing so will enable us to rehabilitate the substrate concrete through calcite precipitation and it will make the concrete to re-repair itself if it cracks again.

The effectiveness of such a product depends on immobilizer that ensures an efficient bacterial metabolism that the cracks in underlying concrete are also repaired by calcite precipitation of the bacteria in it. The material selected as an immobilizer must be natural, abundant and preserves bacteria for a longer time.

Once the concrete cracks, its permeability increases and various aggressive ions along with water penetrates concrete and effect the embedded reinforcement through corrosion. Repairing the crack decreases its permeability and preserving the reinforcement against corrosion but its extent still needs more research for different techniques.

CO₂ is consumed by bacteria to precipitate calcite during its metabolic activity that essentially fills the cracks. However, there are different materials that are being

used as a bacterial immobilizer and adsorbs CO₂. So, it is important to quantify the CO₂ sequestration ability due to calcite precipitation and immobilizer.

1.6 Objective

1. To devise sustainable bio-suspension as repairing agent to damaged concrete
2. To analyze the bond properties and robustness of devised healing suspension against multiple cracking cycles.

1.7 Thesis structure

Followed by introduction, a detailed literature review has been provided in chapter 2 pertaining to self-healing, immobilizers and CO₂ sequestration within the concrete.

Chapter 3 explains the material characterization utilized in the project and in-depth experimental methodology adopted for this research study comprising of casting regime and test numbers.

The results of tests and their critical explanations have been presented in chapter 4 for repairing, healing cycles, corrosion and CO₂ sequestration ability.

The conclusions drawn from this research work and recommendations for future study are summarized in chapter 5 of this thesis

LITERATURE REVIEW

2.1 SELF-HEALING

2.1.1 Characteristics of Repaired Dead Concrete

As, most of the construction that already took place is of dead concrete . there is a big challenge for repairing of the damaged structure. Traditional rehabilitation techniques are expensive and there is durability problem. Most of the durability-related problems of repair systems are due to the lack of compatibility with the concrete substrate. A combination of physical, chemical and mechanical processes results in the failure of concrete repair by H.M. Jonkers et al (2014). a repair material he mortar with bio-based agent shows reduced delamination from the concrete substrate compared to mortar without the bio-based agent. Furthermore, after cracking and healing the mixtures with bio-based healing agent show a slightly better recovery of both flexural strength and deflection capacity from control mixtures without bio-based healing agent (H.M. Jonkers et al (2014)).

Compatibility is another problem while using repairing techniques. Compatibility between the repairs material and the concrete substrate is understood as the balance between deformations and physical and chemical properties of both materials. This balance ensures that the repair system will stand the stresses induced by restrained shrinkage as well as chemical changes (H.M. Jonkers et al (2012)).

So the shrinkage induced in different repairing agents with time were studied by Stefanus Kristiawan (2016) and showed below.

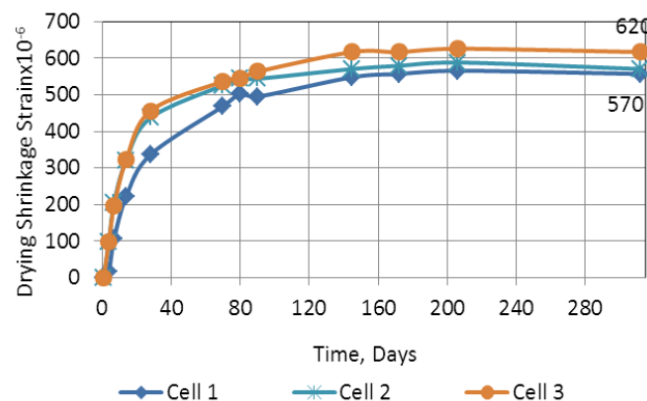


Figure 1: Free shrinkage of PCC with time

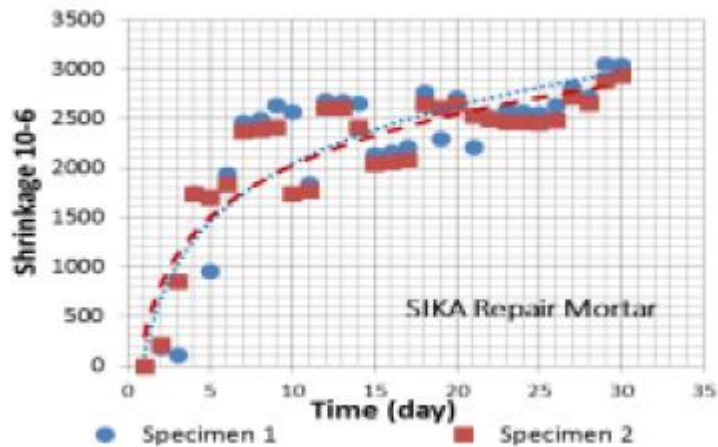


Figure 2: Free shrinkage of Sika Repair Mortar with time

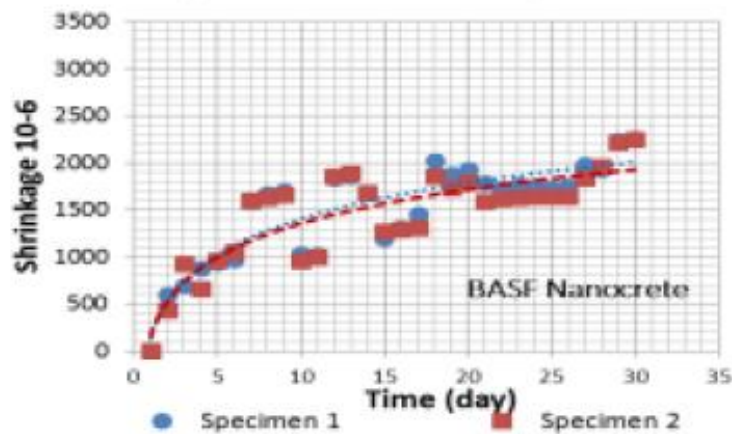


Figure 3: Free shrinkage of BASF Nanocrete with time

It can be seen that both repair materials show similar trend of free shrinkage behaviour that is shrinkage is generally increased with time at diminishing rate. The shrinkage is relatively faster at the beginning of drying so proportional to the lost of water during evaporation and decrease as the time increase. There is differential shrinkage which generate crack again. And again, repair is needed.

2.1.2 Characteristics of Self-Healing Behaviour

Self-healing concrete is manufactured from composite materials that have the capability to assist damaged material in their strength recovery, but the extent of damage directly affects the strength loss (Ghosh, 2005) hence affecting the recovered strength over the course of a structures service life. Since the damage detectability is difficult to predict and structures are vulnerable to sudden failure, self-healing phenomenon is particularly useful in composite material based concrete matrix (Van der Zwaag, 2010).

2.1.3 Classification Based on Self-Healing Behaviour

Based on mechanism involved to repair cracks, self-healing can be classified as either autonomous or non-autonomous (Hager, 2010). Former utilizes external stimuli heat or light for healing action to take place while in latter, damage induced triggers the crack repairing mechanism (Hager, 2010). Another form of self-healing can be intrinsic or extrinsic mode. Extrinsic self-healing involves addition of external agents such as capsules within the cementitious matrix and eruption of these capsules' releases material responsible for crack filling (Van der Zwaag, 2010).

2.1.4 Non-biological Techniques of Self-Healing

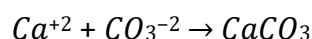
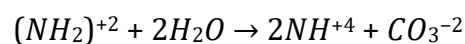
Microencapsulation techniques were adopted in the past researches (Tittelboom, 2011) (Yang, 2007) which essentially involved the release of healing material when the microcapsules busted as result of either change in pH or moisture. Healing agents like epoxy resins (Nishiwaki, 2006), alkali -silica solutions (Mihashi, 2000) were incorporated with cementitious matrix but neither material showed significant strength recovery compared with manual healing mechanisms nor drastically improve the mechanical properties because of permanent voids left at activity site (Tittelboom, 2011).

2.1.5 Bio-Influenced Self-Healing

Bio-influenced self-healing process requires deposition of calcite to fill the micro-structural cracks over period of time and researches have been conducted to analyze the performance evaluation of calcite in enhancement of properties of cementitious matrix (Ramachandran, 2001) (Jonkers, 2007) (Khaliq, 2016).

2.1.6 Biological Process of Microbial Induced Calcite Precipitation

Calcite precipitation potential of bacterial spores is influenced by numerous factors such as surrounding pH, temperature and available nutrients. But the governing factors are 1. Calcium concentration 2. Concentration of dissolved inorganic carbon 3. pH 4. Availability of nucleation sites (Hammes & Verstraete, 2002). The bacteria decompose urea into ammonium and carbonate ions with the help of urease enzyme. The chemical reaction is as follows; (Ng et al, 2012)



The release of ammonium ions via hydrolysis of urea makes surrounding environment more alkaline as result alkaline sensitive bacteria instigate the precipitation of calcite.

Figure 1 shows the schematics of self-healing process of microbial induced self-healing (Hager, 2010)

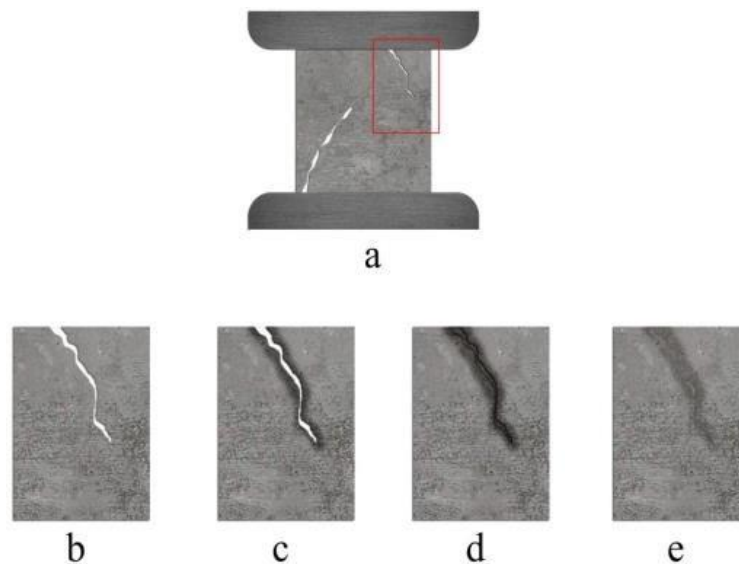


Figure 4: Stages of Crack Healing in concrete

1. Crack is formed under a mechanical load as shown in figure 1.1a
2. Figure 1.1c reflects the general principle, a mobile phase is generated that is triggered by external stimuli which in this case is damage induction.
3. Later, as seen in the figure 1.1d, mass transport takes place at damaged site adhering with crack planes by physical interaction or chemical bonds.
4. Once healing is completed, previously generated mobile phase is attained, with fully restored mechanical properties as shown in figure 1.1e

2.1.7 Bacterial Concentration

Not only does the bacterial type but bacterial concentration also affects the performance of microbial induced self-healing. *E.coli* with 10^5 cells/ml regarded as an ideal concentration to enhance mechanical properties by Ghosh (2007). Ramachandran (2005) has suggested 7.3×10^3 cells/ml for *Bacillus pasteurii* and 6×10^8 cells/ml for *Bacillus psuedofirmus*. For both effective self-healing and enhancement of mechanical properties Nugroho(2015) has suggested 10^5 and 10^6 cells/ml as ideal bacterial concentration for bacterial specie *Bacillus Subtili*

2.1.8 Carrier Materials

Not only bacteria but also its environment in which it exists affect the healing capability of bacteria. So, to study the affect of it, many different types of environment was provided and the bacterial action was observed. The zeolite immobilized bacteria can survive in high pH concrete environment and produce self-healing compounds by Sini Bhaskar et al, (2017). Zeolite is bio compatible and does not damage the bacterial specie.

Self-healing has been advanced in SAP concrete specimen compared to control concrete specimen by Manoj Kumaar. C et al, (2019). Super absorbent polymer(SAP) keeps the bacterial specie dormant.

The zeolite made concrete is capable of absorbing CO₂ by Mengal et al, (2018).

2.1.9 Influence of Nutrients

To precipitate calcite bacterial spores needs an organic precursor for which calcium lactate is considered a suitable choice (Khaliq, 2016), as it starts to dissolve during the mixing process and does not affect the setting time of concrete (Jonkers, 2010).

2.1.10 Improvements in Characteristics

Bacillus Subtilis increased the compressive strength when incorporated with LWA and GNP (Khaliq, 2016). Jonkers (2007) utilized Bacillus psuedofirmus and Bacillus cohnii for microbial induced self-healing and reported a 10% increase in compressive strength. A 17% increase in compressive strength was observed using bacterial specie sporosarcina pasteurii mortar cubes (Achal, 2009).

Sierra Beltran's (2014) evaluation of flexural strength of bio based ECC material concluded a slightly better recovery of flexural strength and deflection capacity of bio-based samples against control samples.

Achal (2011) reported significant reduction in water permeability in cement mortar cubes bearing sporosarcina pasteurii. The reason quoted by Bhasker (2016) was the denser interfacial zone formed between the aggregate and concrete mix via calcite precipitation.

2.1.11 Water-Cement ratio

Water-cement ratio used for our bio influence self-healing bacterial suspension(formulations) is found by using the formula given below (Iman et al , 2014):

$$w/c_{\min} = 0.072 \left(\frac{s}{c} \right)^2 + 0.045 \left(\frac{s}{c} \right) + 0.45$$

2.2 CORROSION

2.2.1 Introduction

Corrosion in reinforcement is an electrochemical process whereby Fe is removed from the reinforcement and dissolves in surrounding water present in the pores of concrete, resulting in the formation of ferrous ions (Fe^+). These ferrous ions then combine chemically with hydroxyl ion (OH^-) and dissolved oxygen (O_2) to form varieties of rust that allows volume of steel to expand by six times (Mansfeld, 1981) generating stresses that initiate cracks resulting in spalling of concrete cover hence reducing the service life of the structure

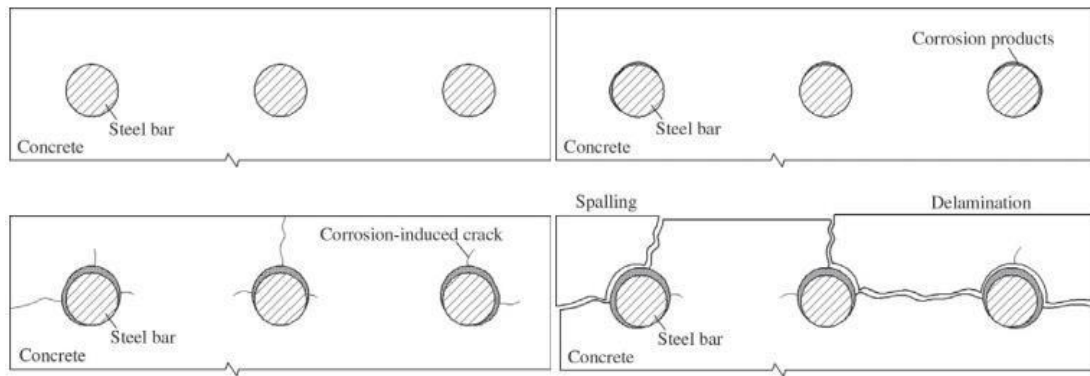
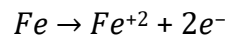


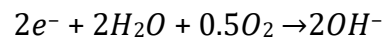
Figure 5: Stages in corrosion induced damage (a) Passive rebar. (b) Corrosion initiation and growth. (c) Further corrosion and crack propagation. (d) Spalling/delamination.

2.2.2 Corrosion Process

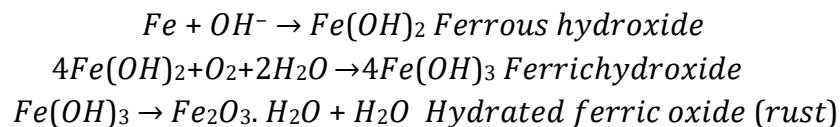
Process of corrosion as illustrated in the figure 3 triggers with the establishment of nucleation sites on steel bar. At anode, oxidation of Fe takes place as per the following equation



Electrons generated travel through the steel to cathode where reduction takes place according to the below equation



Oxygen and moisture utilized in the above equation comes from the permeability of concrete cover and serves as an electrolyte. The formation of rust according to Broomfield (1997) occurs through the following stages



Rust being brittle is reddish brown in colour and its stains can be visible on cracked concrete as well.

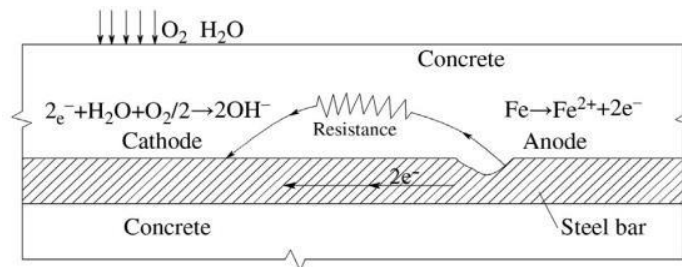


Figure 6: Schematics of corrosion process

2.2.3 Corrosion Rate

An important governing factor regarding corrosion rate is the availability of dissolved oxygen around the cathodic site (Bentur A, 1997). If the supply of dissolved oxygen is not continuous it inhibits the corrosion reaction and for this reason concrete cover is provided for reinforcement as reduces the seepage of dissolved oxygen to prevent corrosion. In such case the rate of corrosion becomes “diffusion controlled” which accounts for decrease in potential between anode and cathode, a process called polarization.

Another significant factor that determines the rate of corrosion is restriction of ionic current passing through the pores of concrete. Slower the flow rate of charge carrying ionic species; lower would be the rate of corrosion reactions and this can be attained by higher electrical resistance of concrete surrounding the rebar. Lastly, a process termed passivation restricts the rate of corrosion. In dense concrete this phenomenon does not occur due to high alkalinity (pH 13) but when the concrete is exposed to pH 11.5 (depicted in the figure below) and above in presence of dissolved oxygen, the rebar reacts with it to form metal oxides/ hydroxides which are thin, dense and impenetrable. This film prevents anodic reaction renders the rate of

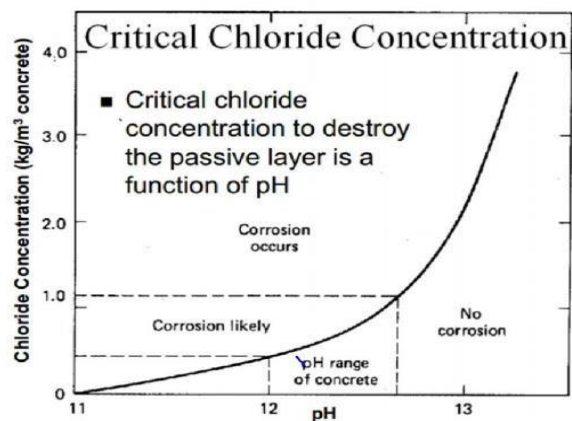


Figure 7: Relationship between Cl^- concentration and pH; Source: Steel corrosion in concrete by Bentur et al

corrosion so slow that in some cases steel can be believed to be non-corroding. However, the breakdown of this passive layer can take place due to ingress of chloride ions or carbonation. It is worthy to mention that chloride and carbonate ions diffuse into concrete without significantly damaging it unlike sulphate ion that deteriorate concrete without harming steel.

The service life of reinforced concrete structures can be divided into two stages, the initiation stage and the propagation stage illustrated through the graph in the figure below. In the first stage reinforcement is passive but de-passivation due to chloride attack and carbonation results in corrosion. Adequate concrete cover and reduced penetration rate of above-mentioned aggressive agents prolongs the initiation stage. The second stage begins after de-passivation and end after limit state is attained whereby, the cracking of steel or spalling of concrete occurs.

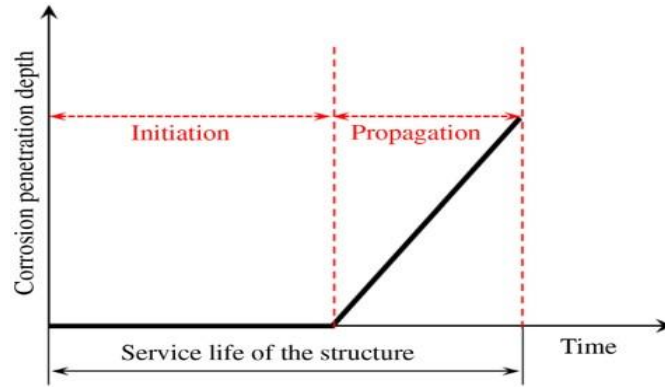
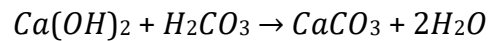
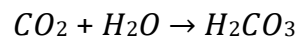


Figure 8: Relationship between Corrosion penetration depth and service life of structure

2.2.4 Carbonation-Induced Corrosion

Carbonation within the concrete causes neutralization of its alkalinity that disturbs the stable passive layer protecting the reinforcement. Carbonation starts near the surface of concrete and slowly propagates towards the inner zones reaching near-neutral pH levels through the following equations



CHAPTER 3

MATERIAL AND EXPERIMENTAL METHODOLOGY

3.1 MATERIALS

Materials used in manufacturing of CO₂ inhaling bio healable concrete as well as their characterization are mentioned in the upcoming section followed by a detailed experimental methodology.

3.1.1 Zeolite

Zeolite we procured was from Chitral. The zeolite obtained was in rock form, we carry out grinding and raw powder form was obtained. We conducted sieving and #200 passing was obtained. We performed particle size analysis (PSA) and the results are shown below:

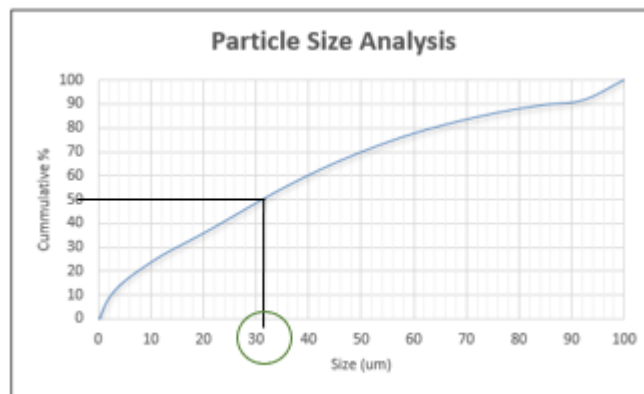


Figure 9: Particle Size Analysis of Zeolite

Here, median size is 31 micrometers. We also did XRF and found out the percentages of different compounds in zeolite.

Table 1: Compound in Zeolite

%	SiO ₂	Al ₂ O ₃	CaO	MgO	SO ₃	K ₂ O	Na ₂ O	Fe ₂ O ₃
Zeolite	57.6	12.4	2.93	.43	.72	2.73	12.14	.78

3.1.2 SAP (Super Absorbent Polymer)

SAP (super absorbent polymer) was ordered online. We also did the Particle size analysis of it and we found out its median size(d_{50}). The PSA curve is given below:

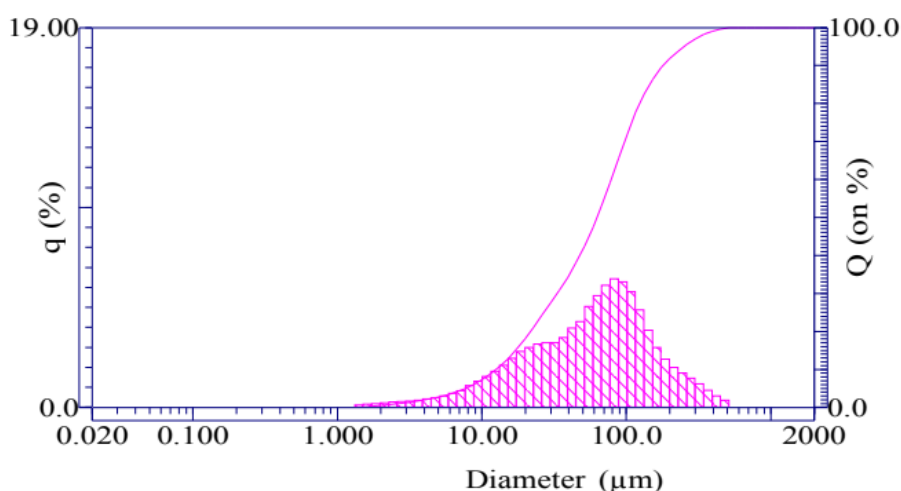


Figure 10: Particle Size Analysis of SAP

Table 2: Properties of SAP

Median	62.6172 μm
Mean	83.3575 μm
Variance	79.3255 μm

3.1.3 Bacteria

Bacteria utilized in the research study was bacillus subtilis which is a rod shaped, gram-positive bacterium found commonly in soil. It has the ability to resist extreme pH and temperature yet forming protective endospores.

Bacillus subtilis used has American type culture collection (ATCC) number 11774 and is manufactured under ISO 9001:2008 certification. Nutrient broth used for bacteria consisted of lab-lemco powder 1.0 g/l, yeast extracts 2.0 g/l, peptone 6 g/l and sodium chloride 5.0 g/l. pH 7 ± 0.2 . All cultures were incubated aerobically at 37°C for 24 h with shaking at 250 rpm. The pure culture was maintained in liquid, on nutrient agar plate, and cryopreserved in 80% glycerol at -80°C .

The growth of bacterial spores was done in ASAB microbiology lab, where a fixed concentration of bacteria to be added was attained. For verification, a reference blank solution was prepared and absorbance of bacteria was noted through spectrophotometer. A selected wavelength of 600 nm was applied on a 0.5 ml blank

solution and after the machine had detected the blank solution it was replaced with 0.5 ml bacterial solution with again same wavelength applied over it. Ramachandran equation $Y = 8.59 \times 10^7 \times X^{1.3627}$ where “Y” is concentration of bacterial solution in cells/ml and “X” is optical density (OD) obtained from spectrophotometer. The bacterial concentration in our case was selected to be 3.3×10^7 cells/ml for casting of concrete.

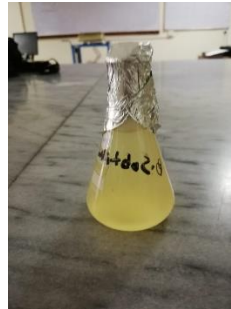


Figure 11: Prepared solution of bacillus subtilis

3.1.4 Calcium Lactate

Calcium lactate act as a food for bacteria in the precipitation of CaCO_3 and has been widely used in self-healing studies as reported in literature (Jonker, 2010) due to its ability to dissolve readily during mixing phase of casting. Calcium Lactate

Pentahydrate was of DAEJUNG (CAS # 5743-47-5, CAT # 2513-4405) with its properties summarized in the table below

Table 3: Properties of calcium lactate

Linear Formula	$\text{C}_6\text{H}_{10}\text{CaO}_6 \cdot 5\text{H}_2\text{O}; \text{Ca}(\text{CH}_3\text{CHOHCOO})_2 \cdot 5\text{H}_2\text{O}$
Molecular Weight	308.3
Assay	98%
Melting Point	240 °C

3.1.5 Cement

Bestway grade 53 cement, preserved in a sealed container from moisture, was used in our research study. The table below lists the properties of cement.

Table 4: Properties of cement

Median Size (D50) (μm)	9.50
Final Setting (min)	135.0
Specific Gravity	3.14
Initial Setting (min)	35

3.1.6 Sand

Lawrencepur sand was used in our research bearing a fineness modulus of 2.55 which is well within the prescribed limits (2.2 to 3.2) of ASTM. The gradating curve shown in the figure below was obtained by performing the sieve analysis according to ASTM C33.

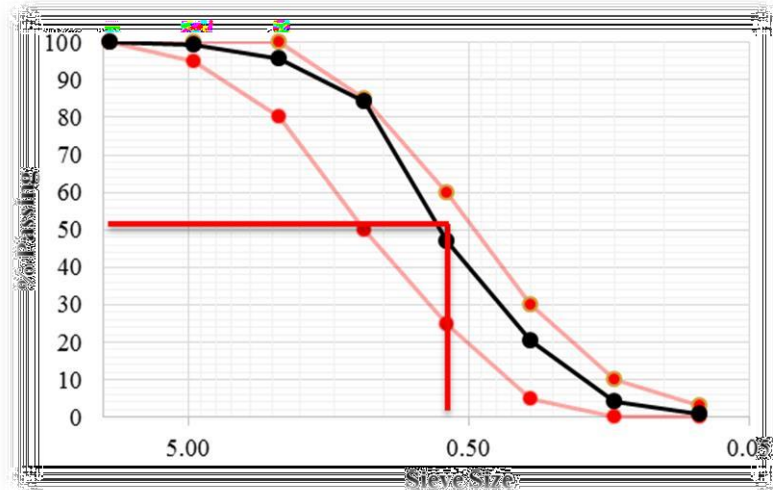


Figure 12: Particle size distribution of sand

Table 5: Properties of sand

Median Size, (D ₅₀) (mm)	0.595
Fineness Modulus	2.54
Specific Gravity	2.81
Water Absorption	0.54%

3.1.7 Aggregate

The aggregate was procured from Margalla and the following table summarizes the properties of aggregate.

Table 6: Properties of aggregates

Crushing Value	21.6%
Specific Gravity	2.679
Water Absorption	1.08%

3.1.8 Steel

Karachi steel was used in our research project having following properties

Table 7: Properties of steel

Bar Size	4
Grade (ksi)	40
Yield Strength (Mpa)	355.9

3.2 EXPERIMENTAL METHODOLOGY

In order to investigate the objectives established for our research study we conducted a series of tests on 81 different concrete specimens. The table below lists the test numbers for the research work.

Table 8: Details of casting

Test	Moulds	Quantity	Formulations	Total
Bio-Healing	Cylinders (4"x 8")	11	5	55
CO ₂ Monitoring	Cylinders (4"x 8")	8	2	16
Corrosion	RCC Cylinders (4"x 8")	1	5	5
Healing Cycles	Cylinders (4"x 8")	1	5	5
Total				81

Concrete samples were repaired using 5 formulations that were Non Bacterial Grout (NBG) which is a normal cement grout, Bacterial Spray (BS) which is in liquid form and a mixture of nutrient and bacterial solutions in specified proportions, Bacterial Grout (BG) which is a cement grout which bacteria and nutrient added to it but no immobilizer, SAP immobilized bacterial grout (BSAP) which is same as BG with SAP as immobilizer added to it, Zeolite immobilized bacterial grout (BZ) which is same as BG with zeolite as immobilizer added to it.

3.2.1 Mix Design

In order to formulate the mix design of concrete, the design compressive strength of concrete was taken to be 4000 psi and the properties of the constituents were used as illustrated previously. The mix design of concrete was formulated using ACI design method.

Table 9: Details of concrete mix design

Sample Name	Cement	Fine Aggregate	Coarse Aggregate	Water
Concrete	1	1.71	2.67	0.47

In order to formulate the mix design of different formulations, literature was referred. A bacterial solution was prepared with 10^5 - 10^6 cell/ml concentration of bacillus subtilis. A nutrient solution was also prepared with calcium lactate having concentration of 0.5% of cement. Zeolite was kept 10% to the weight of cement.

SAP was kept as 0.2% of weight of cement. However, both these quantities were consulted from literature

Table 10: Mix Designs of formulations of grout

Details of Formulations						
Formulations	Ingredients					
	Cement	Water	Zeolite	SAP	Nutrient Solution	Bacterial Solution
NBG	1	.45	-	-	-	-
BS	-	-	-	-	.225	.225
BG	1	-	-	-	.225	.225
BZ	1	-	.1	-	.225	.225
BSAP	1	-	-	.002	.225	.225

3.2.2 Mixing Regime

Following mixing scheme, summarized in the table below, was employed for casting of concrete and grout done using concrete mixer and Hobart mixer of NICE structures lab.

Table 11: Procedure for normal concrete preparation

Step 1	The materials were weighed as per the mix design
Step 2	Cement, sand, aggregate was slow dry mixed for 45 sec
Step 3	80% water was added to the dry mix whilst mixing shaft slowly rotating for a period of 90 sec
Step 4	Remaining water was added during the fast mixing process that lasted for 45 sec
Step 5	The concrete mix was poured into the moulds
Step 6	The moulds were placed on vibrating table for even compaction and the surface was levelled with trowel

Grout was mixed using the standard procedure from ASTM C 778, which is used for mixing hydraulic cement paste and mortar. Materials were weighed and added into the mixture for different formulations according to the mix design. BS was

prepared through hand mixing of nutrient and bacterial solution according to the specified proportions.

Table 12: Procedure for grout preparation

Step 1	The materials were weighed as per the mix design. Hobart mixture was used for grout preparation
Step 2	Bacterial and nutrient solutions were placed into the bowl
Step 3	Cement, calcium lactate and immobilizer were added according to the mix design of formulations and allowed 30 sec for absorption
Step 4	Hobart mixture was started at slow speed for 30 sec
Step 5	Mixture was stopped for 15 sec to scrap down any grout stuck on sides
Step 6	Mixture was started at medium speed and mixed for 60 sec

3.2.3 Curing

After the normal concrete specimens were casted, they were demolded after 24 hours and placed in the temperature-controlled curing tank at 25°C for 28 days before being ready for cracking.

When the grout was applied to the cracks of the normal concrete it was left to dry for 24 hours and then repaired concrete samples were again cured in the same curing tank for 3,7,14 and 28 days before being ready for testing.

3.2.4 Application

We had five formulations. NBG, BS, BG, BZ and BSAP, out of these five formulations, four are grout while BS is suspension. In order to apply these formulations, we used injection for grout and spray bottle for BS, injection selected was based on its nozzle size and for our suspension we used a normal spray bottle, their figures are given below:



Figure 13: Pictorial representation of Application

The grout was applied between the cracks of the cracked samples. The suspension was sprayed over the cracked samples using spray bottle.

EXPERIMENTAL TESTS AND RESULTS

4.1 HEALING ANALYSIS

4.1.1 Crack Width Measurement Analysis

CWMA is a visual technique whereby crack filling by microbial precipitation within the concrete samples is recorded using optical microscope. It was only performed on the samples treated with bacterial spray as grouts covers the crack. The samples were cracked, and bacterial spray was sprayed and then they were re-cured for 28 days after which they were inspected for crack healing potential as summarized in the table below.

Table 13: Summary of CWMA results

SAMPLE	28D 28D
BS	2 mm

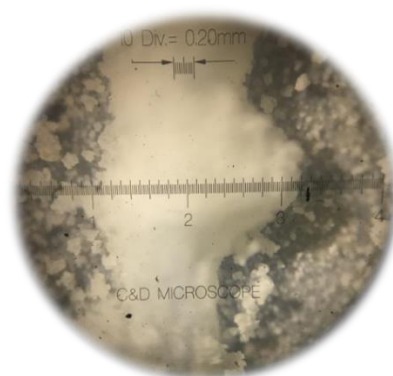


Figure 14: OM image of BS

The deduction from the CWMA test result is that the healing has being observed in case of BS samples with the maximum crack width healed is 2 mm. hence validating the bacterial activity. So, we can say that by using our bacterial spray, the dead concrete can be converted into smart live concrete.

4.1.2 Thermogravimetric Analysis

TGA is thermal analysis technique to identify different crystalline compounds in the cementitious matrix based on their decompositions at different temperatures. The change in mass in accordance with an increase in temperature, from 0 to 800°C gives the quantity of crystals of compound present. It is mentioned in literature that the calcite decomposes at 525 to 800 °C. So, The TGA plot of our two suspensions (BS, BG) were analyzed. From 100 to 600 °C refers to ettringite that is a hydration product of concrete. Isfahani (2016) in his research findings identified temperature range from 400 to 500 °C for portlandite mass loss. Moreover, Warda Ashraf (2017) quoted 773.2 °C to be calcite burning temperature. We investigated temperature range 500 – 800 °C, the percentage change in the mass was observed referring it to amount of calcite present within the different concrete formulations.

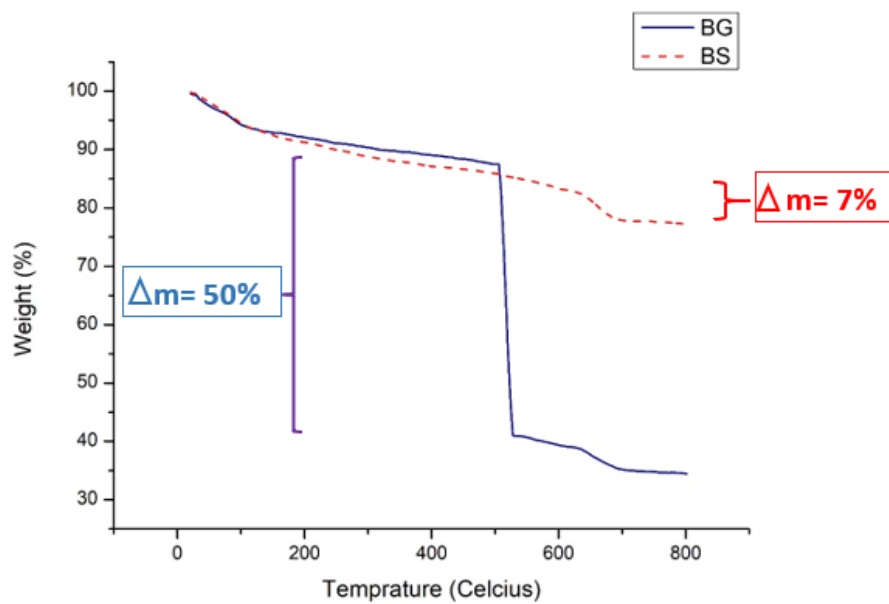


Figure 15: TGA of BG and BS

The change in the mass (50% & 7%) in the temperature region 500-800 °C BG and BS respectively, corresponds to calcite decomposition.

4.1.3 X-Ray Diffraction Analysis

XRD analysis is the phase identification of crystalline material to distinguish elemental components in repaired concrete. For this test, a small sample (5 – 10 g) was extracted from repaired samples and analyzed. So, relative peaks corresponding to specific elements is obtained.

XRD analysis was performed for all four suspensions (BS , BG , BZ , BSAP) and the results were analyzed. Following are the XRD of suspensions:

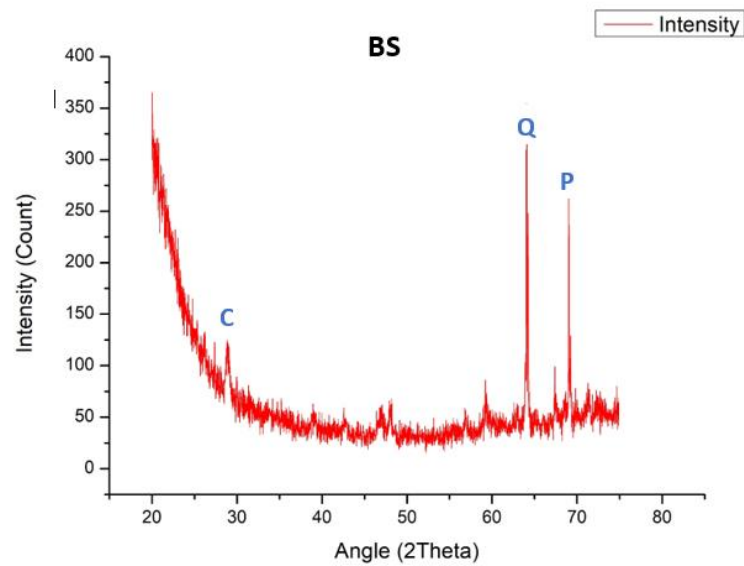


Figure 16: XRD of BS

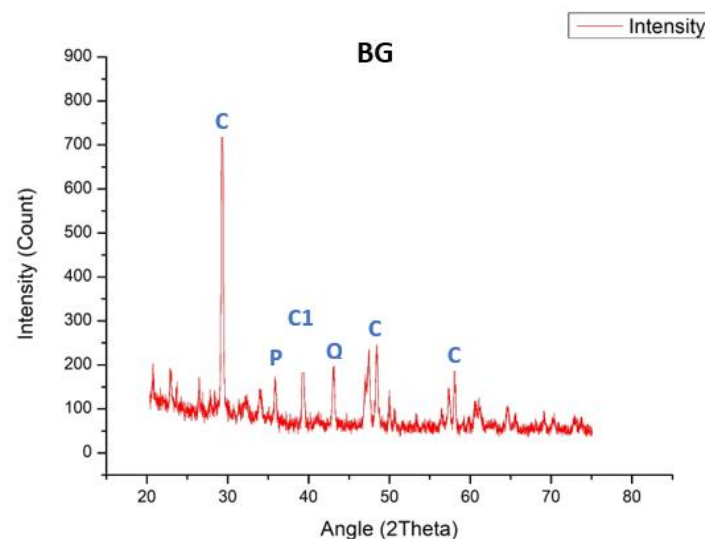


Figure 17: XRD of BG

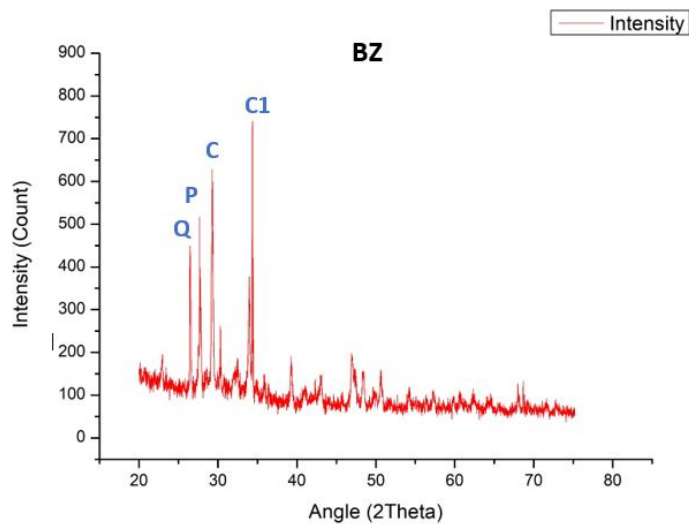


Figure 18: XRD of BZ

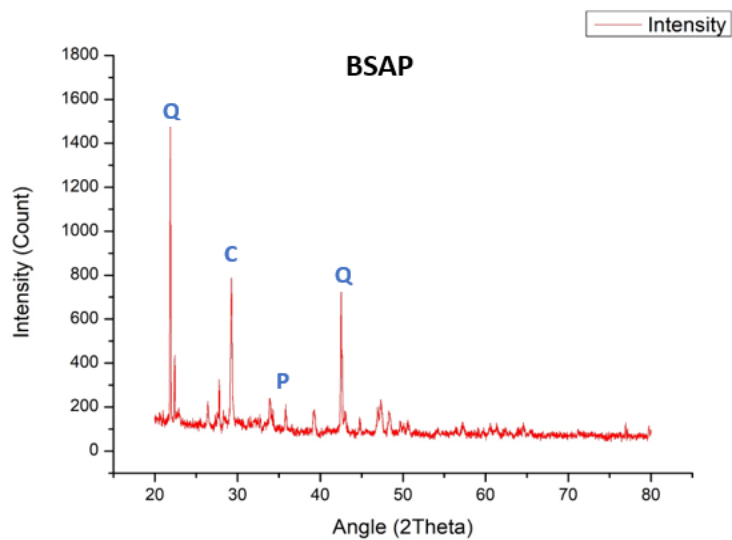


Figure 19: XRD of BSAP

Label	Name	Formula	Crystallography
Q	Quartz	SiO ₂	Hexagonal
P	Portlandite	Ca (OH) ₂	Hexagonal
C	Calcite	CaCO ₃	Rhombohedral
C1	Aluminium Silicate (Kyanite)	Al ₂ SiO ₅	Triclinic

Figure 20: Compounds identified using XRD analysis

We can clearly see the peaks at phase (29.93°) in XRD analysis of all suspensions indicating the presence of calcite precipitation. It can be related to the bio-metabolic activity which is induced by applying our suspensions.

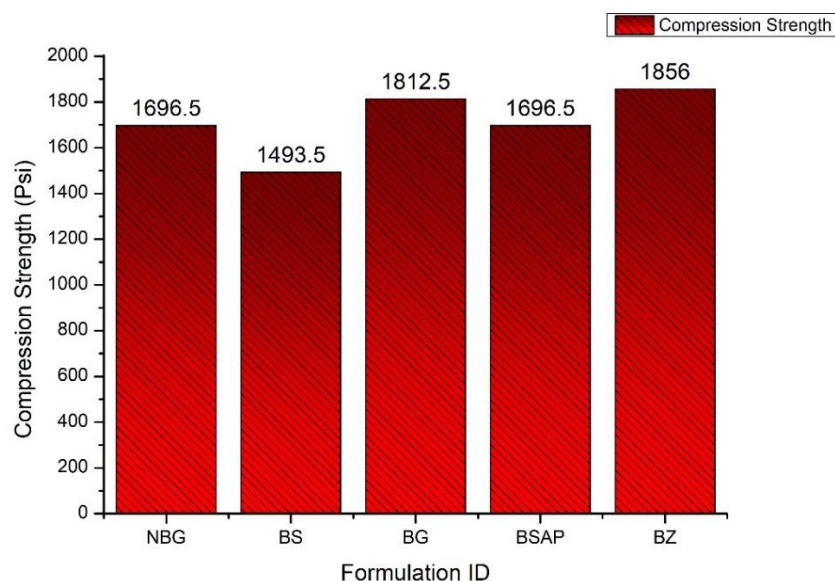
4.1.4 Strength Recovery Index

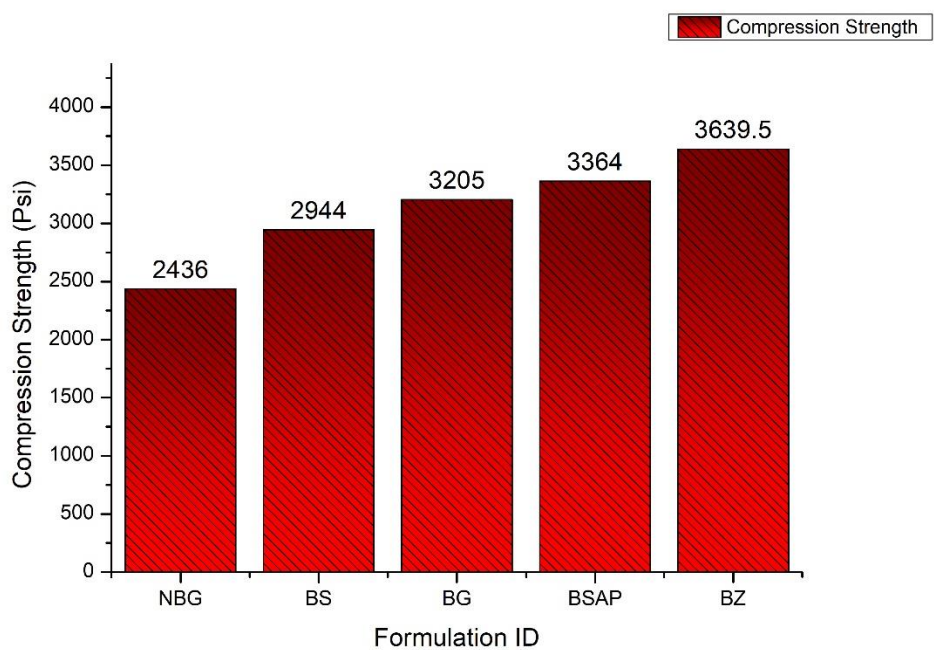
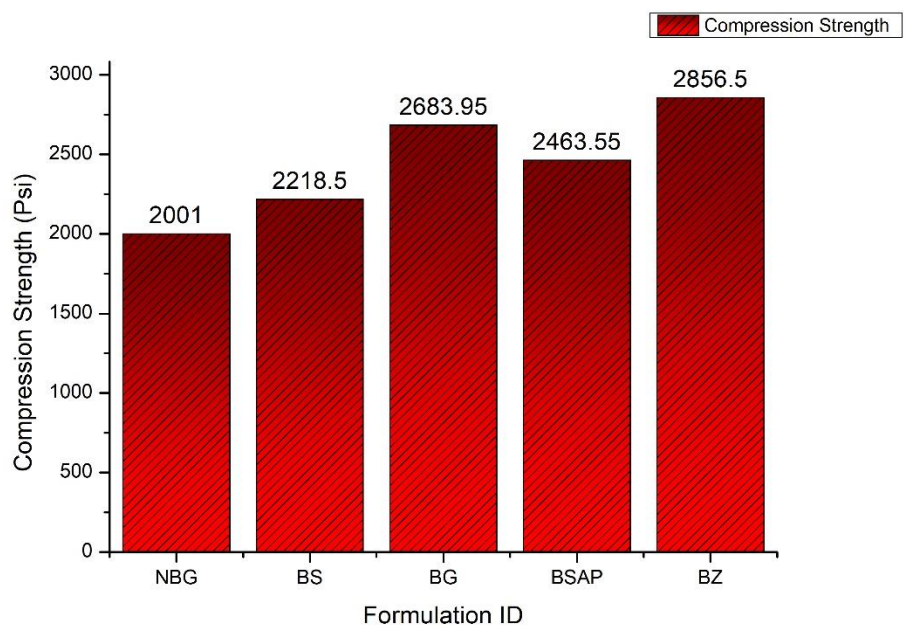
Bacterial suspensions not only fill and heal the concrete cracks but has the potential to restore the mechanical properties such as its tensile and compressive strength, lost due to cracking. Strength recovery index (SRI) represents regain of respective strength after healing action in terms of percentage of its initial strength using the following formula.

$$SRI = \left(1 - \frac{\text{Initial Strength} - \text{Required Strength}}{\text{Initial Strength}} \right) \times 100$$

SRI was calculated for both the compression strength and tensile strength.

Start with the compression strength, the graphs below show the compressive strengths of the healed concrete samples at curing periods of 3, 7, 14 and 28 days, respectively. It was observed that with introduction of our suspensions the healing efficiency has improved that results in densification of concrete matrix enabling it to withstand increased loads with maximum regain strength for BZ.





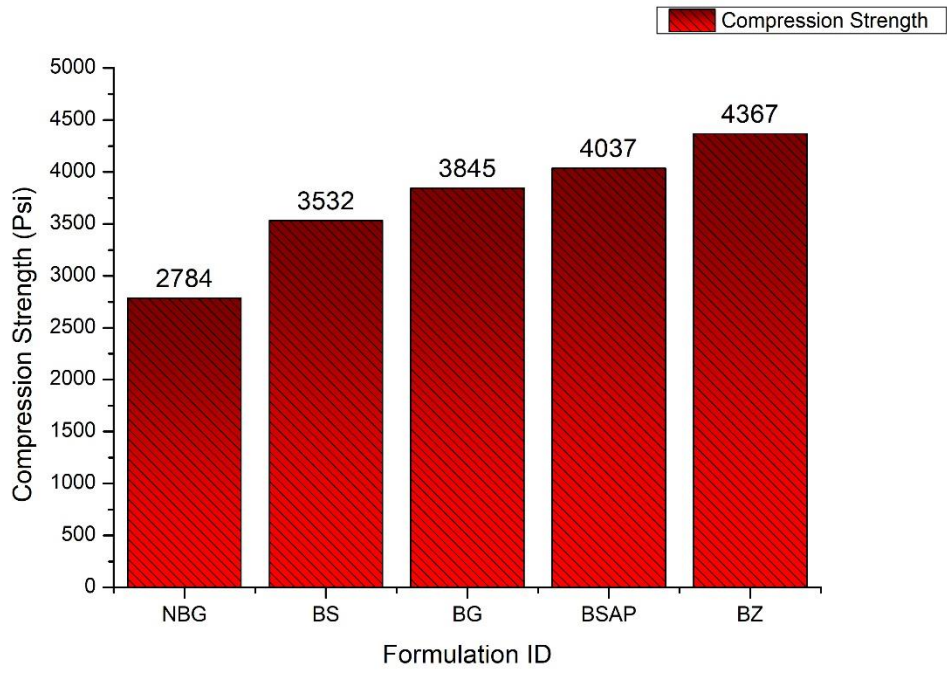


Figure 21: Compressive strengths at (a) 3 days (b) 7 days (c) 14 days (d) 28 days, of cured samples

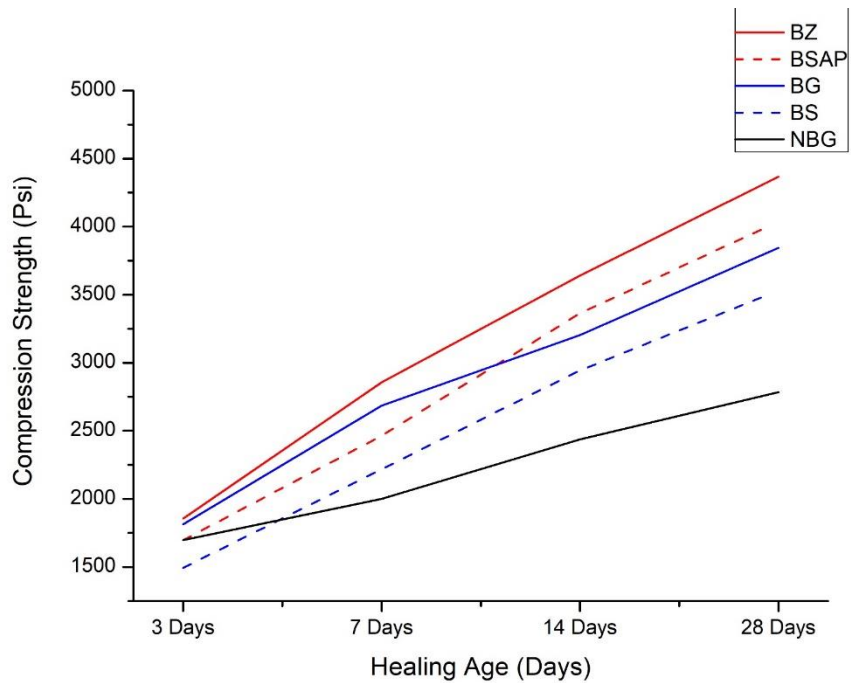


Figure 22: Compressive strengths recovery rate with healing age, of cured samples

Generally, if we analysis the results we can see that the compression strength recovered in the healed samples ranges from 60 to 90 % of its initial strength. The matrix figure below shows strength recovered against respective cured periods. The maximum of 96.7% strength recovery was observed for BZ.

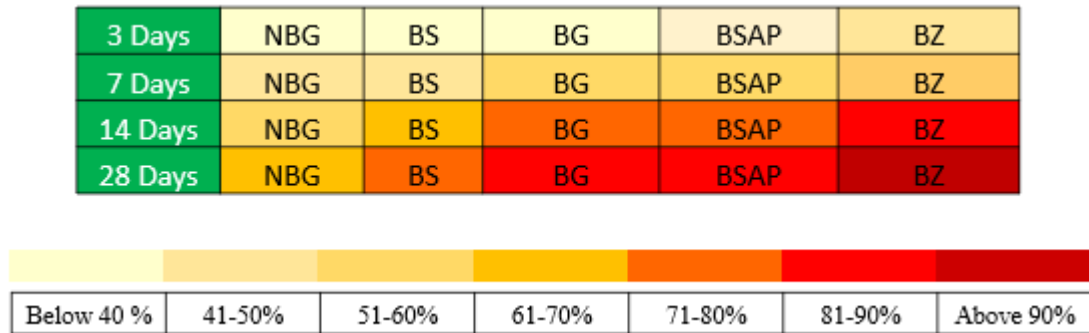
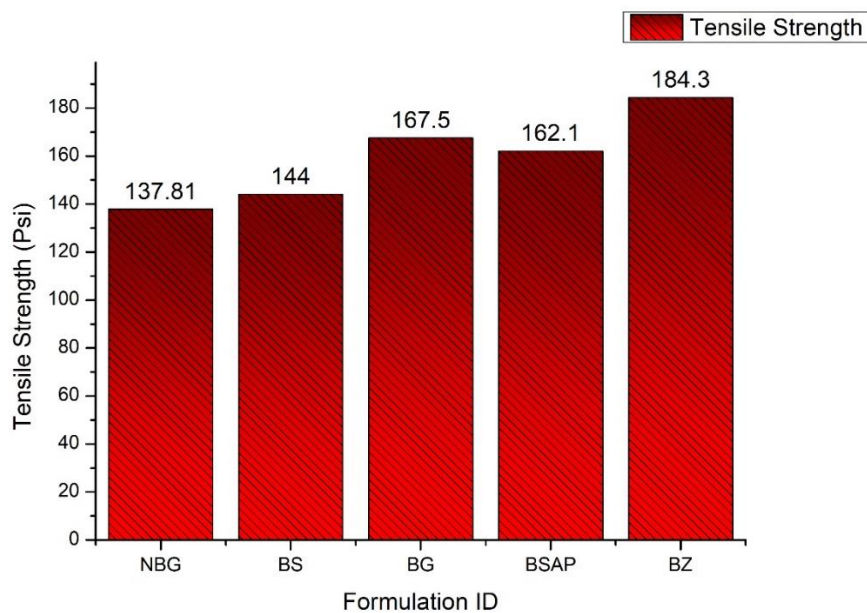
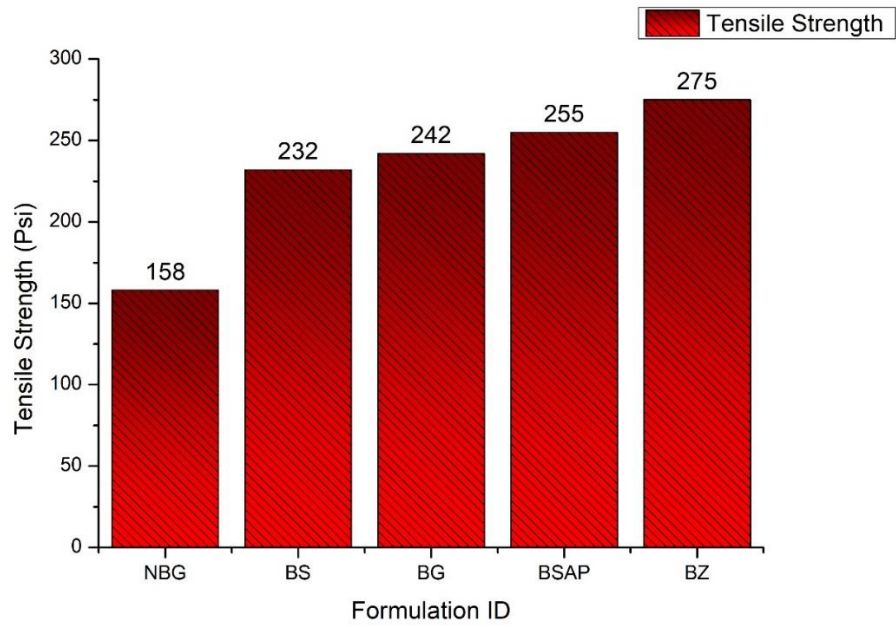
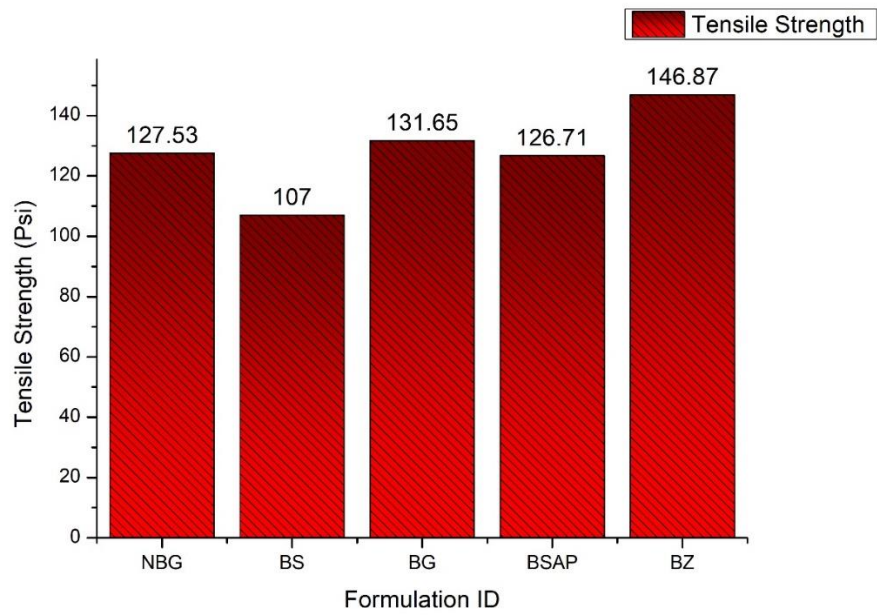


Figure 23: Compression Strength recovery matrix for different formulations

Now SRI for the tensile strength, the graphs below show the tensile strengths of the healed concrete samples at curing periods of 3, 7, 14 and 28 days, respectively. Here also it was observed that with introduction of our suspensions the healing efficiency has improved that results in densification of concrete matrix enabling it to withstand increased loads with maximum regain strength for BZ.





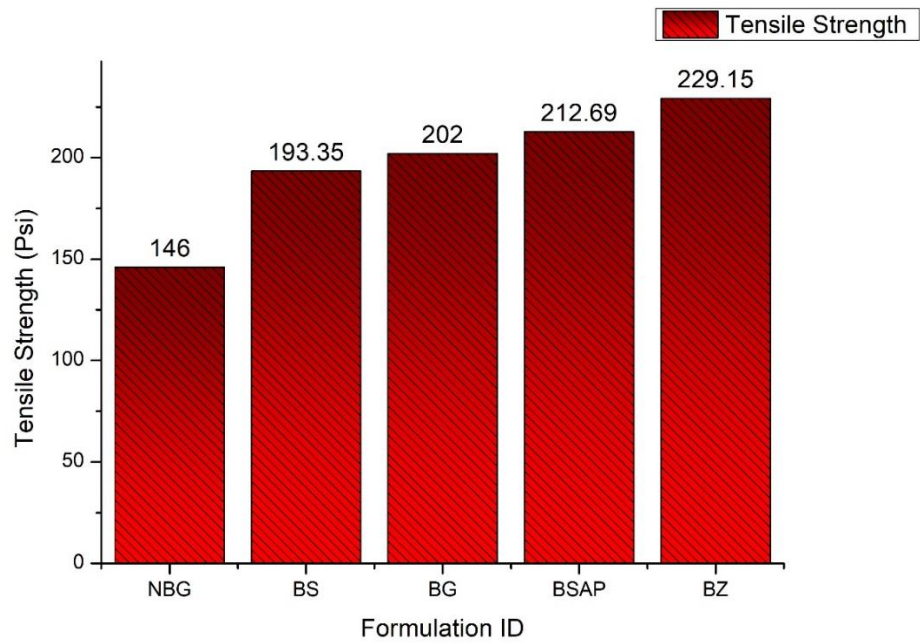


Figure 24: Tensile strengths at (a) 3 days (b) 7 days (c) 14 days (d) 28 days, of cured samples

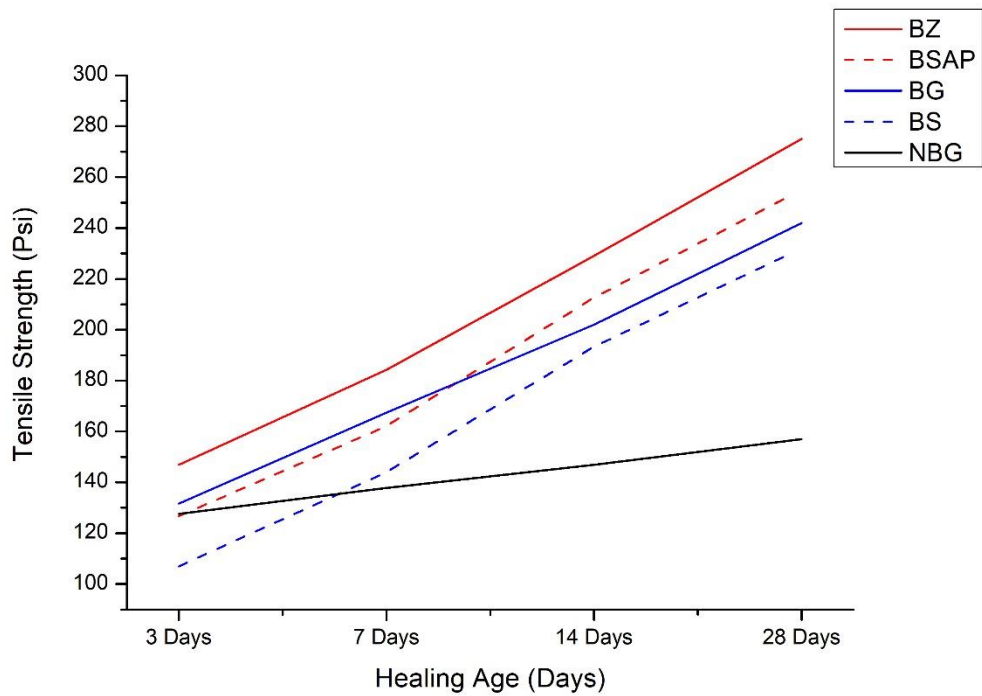


Figure 25: Tensile strengths recovery rate with healing age, of cured samples

Generally, if we analysis the results we can see that the tensile strength recovered in the healed samples ranges from 60 to 90 % of its initial strength. The matrix figure below shows strength recovered against respective cured periods. The maximum of 92.3% strength recovery was observed for BZ.

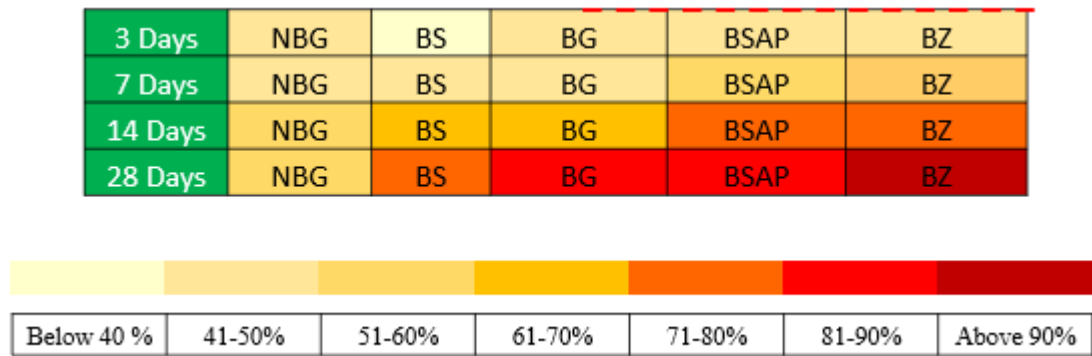
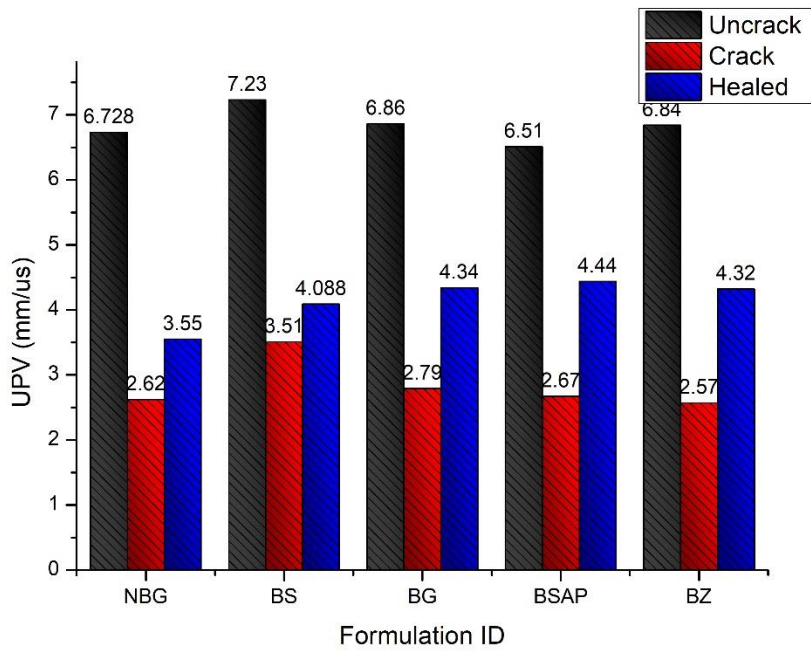
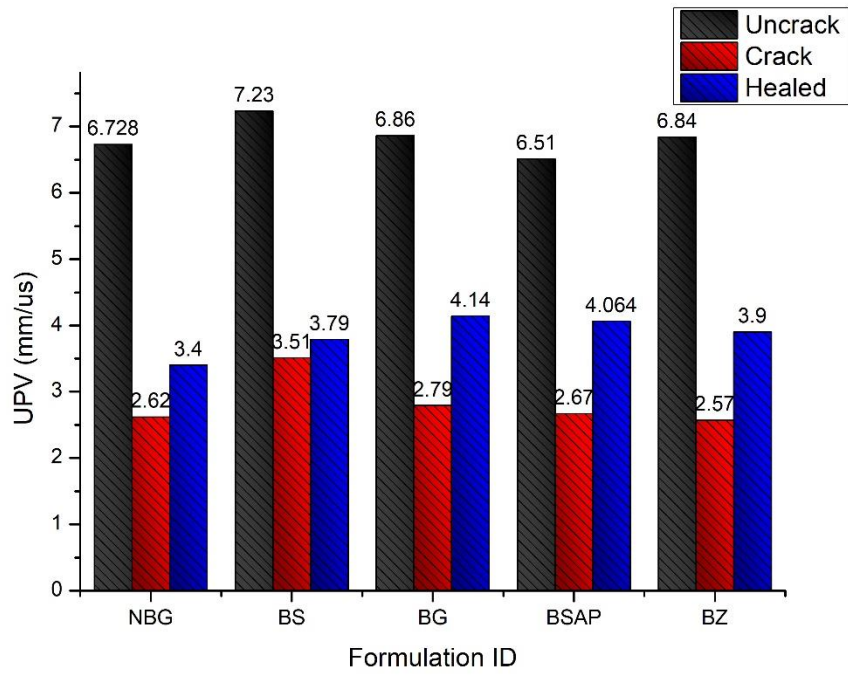


Figure 26: Tensile Strength recovery matrix for different formulations

4.1.5 Ultrasonic Pulse Velocity

UPV test was carried to monitor the healing activity within the concrete samples cured at respective periods after the application of our suspensions, for which the internal cracks were filled. In order to estimate the healing activity UPV was performed before cracked, then for pre- cracked and later for repaired samples at four different healing period (3 days, 7 days, 14 days and 28 days). The direct method was employed to investigate healing. It was observed that the velocity increase with the healing age as the cracks start healing and the internal discontinuity due to internal cracks decreases. The following graphs depicts the velocities through concrete samples at different healing period:



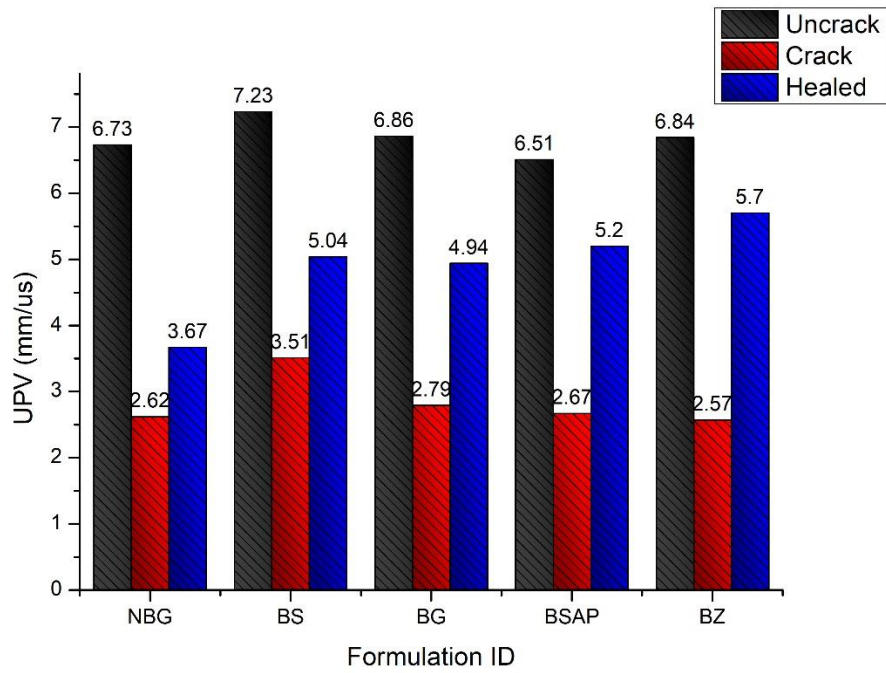
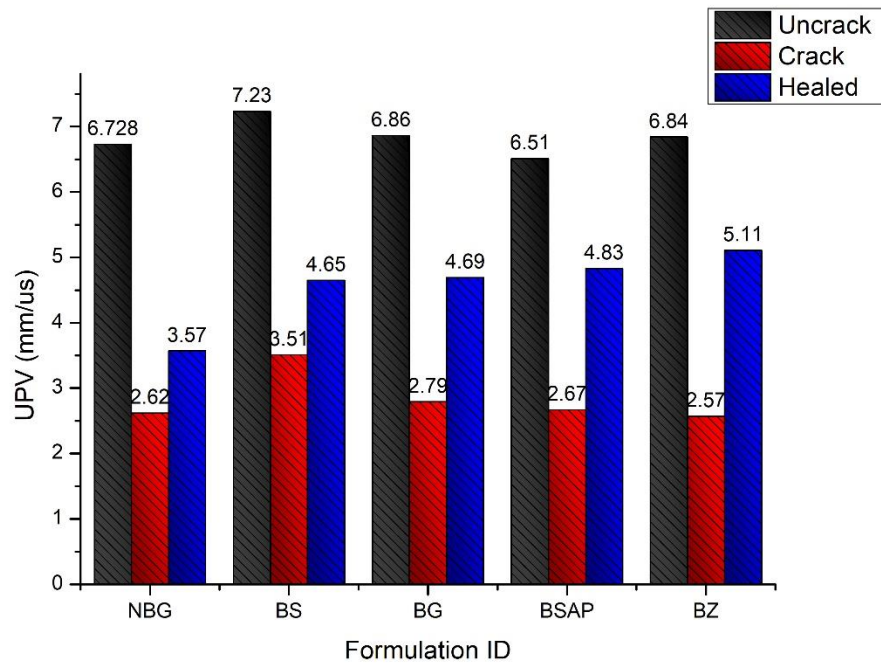


Figure 27: UPV on (a) 3 days (b) 7 days (c) 14 days (d) 28 days, uncracked, cracked and healed samples

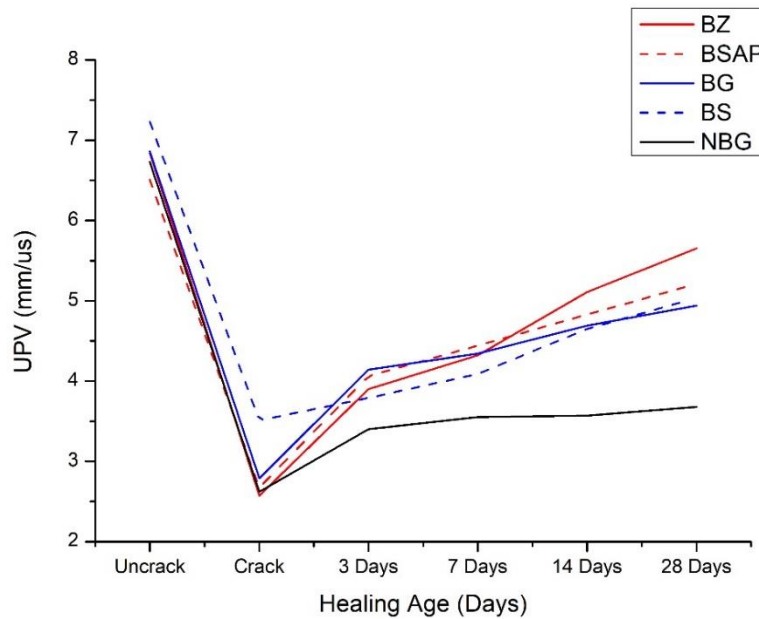


Figure 28: UPV recovery rate with healing age, of cured samples

The results of UPV compliment the previous test results that were performed to check the healing capability of our suspensions. It can be seen that with increase in healing age, the UPV velocity increases indication that healing is taking place in samples on with our bacterial suspensions were applied as compare to NBG. Among all of them BZ gives the best results with the UPV of healed sample is 83.3 % of uncracked sample.

In mechanical method, the sponge was used to remove the corrosion products. In chemical method, the bars were immersed in 20 % w/w solution of NaOH with 2% granulated zinc for 40 minutes at 85°C according to the standard ASTM G1-03.

4.2 CORROSION

4.2.1 Weight Loss Measurement

Weight loss measurement is a classical technique to determine the corrosion rate of the rebar in the concrete samples. Weight of the rebars before casting was noted using balance with accuracy of up to 0.1 g. The same cylindrical samples with rebar at its center were casted and were placed for curing. After the 28 days curing period, the samples were dipped in 3.5% NaCl solution and a DC supply of 12 V was applied for 12 hours. The Samples were then broken down and the corroded bars were cleaned using both mechanical and chemical methods.



Figure 29: Pictorial description of weight loss measurement test

The weights of bars after washing was measured and change in mass of the bars were calculated to find the percentage of corrosion for different formulations as shown in the following graph.

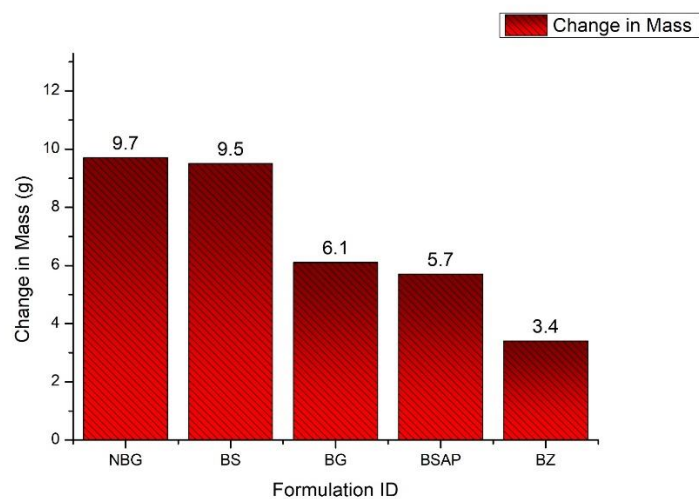


Figure 30: Weight loss measurement results

The change in mass corresponds to the amount of corrosion in the concrete specimens with maximum corrosion observed in case of specimen on which NBG was applied and least evident in BZ (almost 65 % less as compared with NBG) with only 1.13 % decrease in rebar weight. The test result also supports the hypothesis of healing of concrete repairing micro-cracks reduces the concrete impermeable to chloride and carbonation agents which triggers corrosion in the embedded concrete reinforcement. And it can be seen in the graph showed above.

4.3 CO₂ Monitoring

4.3.1 Climate Controlled Chamber

The amount of CO₂ absorbed by different formulations was to be measured, but the scope had to be minimized due to Covid-19 and only NBG and BZ were tested, as research shows that along with CO₂ sequestration due to calcite precipitation zeolite adsorbs CO₂. A customized climate control chamber was assembled with its schematics displayed in the following figure

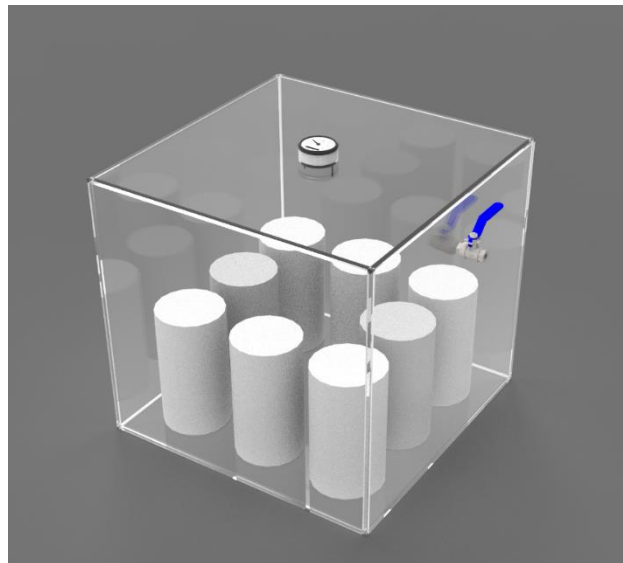


Figure 31: Schematics of climate control chamber



Figure 32: Real time CO₂ monitoring in the climate control chamber

As seen, chamber is a cuboid having a length, width, and height of 1.5 feet made of 6 mm acrylic glass. Mounted on the top is EXTECH sensor that records CO₂, humidity and temperature with time. The sensor can be time calibrated with minimum stage of 1 minute with its probe suspended inside the chamber. The sensor was set at a stage of 10 minutes. The sensor comes along with a data logger that continuously records the readings, as per the stage set, in an excel file which can be retrieved through the memory card fitted inside the sensor.

On one of the sides of the chamber, a 0.25 in diameter valve was installed for the entry of CO₂. CO₂ gas was inserted through a CO₂ cylinder and it was inserted in the chamber till the value of CO₂ concentration as recorded by EXTECH meter became 4000 ppm.

To ensure that the entrapped CO₂ gas does not leak into atmosphere the sides of the chamber were lined through silicon sealant both internally and externally, in addition to it, the external edges were covered with scotch tape. Eight cylindrical concrete samples of dimensions 4” diameter and 8” height was placed in the chamber of NBG and BZ formulations.

The underline methodology was to raise the concentration of CO₂ within the chamber up to maximum of 4000 ppm and monitor changes in concentration to reach a minimum threshold of 100 ppm. The graph below shows the concentration of CO₂ against time for NBG and BZ formulations.

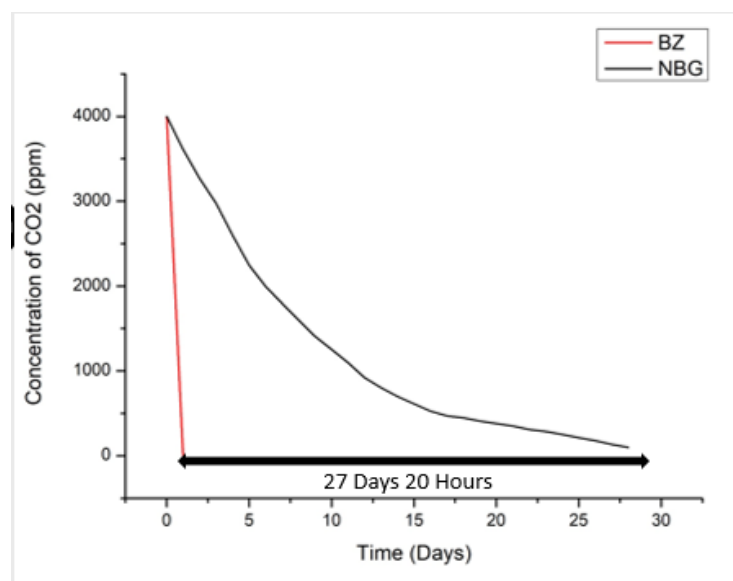


Figure 33: CO₂ monitoring result extracted from sensor

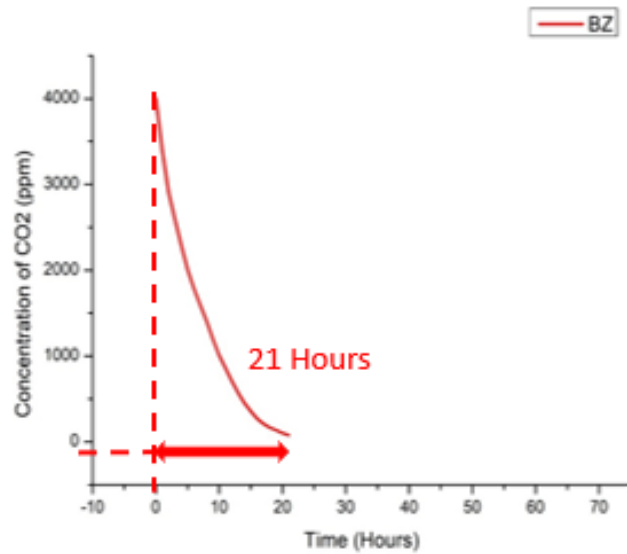


Figure 34: CO₂ monitoring result of BZ extracted from sensor

The NBG sample took 27 days and 20 hours to reach a point of 250 ppm which implies that it has reached its maximum ability to absorb CO₂. Moreover, this intake of CO₂ is detrimental to concrete as it causes carbonation and reduces alkalinity of concrete which leads to corrosion as evident from phenolphthalein test result shown in the figure below. The purple area represents section unaffected by carbonation whereas grey area shows section affected by carbonation.



Figure 35: Phenolphthalein Test for NBG

With the introduction of zeolite as immobilizer, the CO₂ sequestration ability of concrete has increased drastically as can be inferred from the above graph that the BZ has the highest potential to inhale CO₂ taking only 21 hours to reach minimum threshold of 100 ppm. The phenolphthalein test shown in the figure below testifies that this absorption of CO₂ was not as a result of carbonation but due to micro-bacterial calcite precipitation and CO₂ adsorbed by zeolite.



Figure 36: Phenolphthalein test for BZ

4.3.2 Room Model

In order to study the environmental impact of bacillus suspended grout reasonably it is imperative to model a hypothetical room that was plastered using bacterial zeolite grout (BZ) was designed as displayed in the figures below.

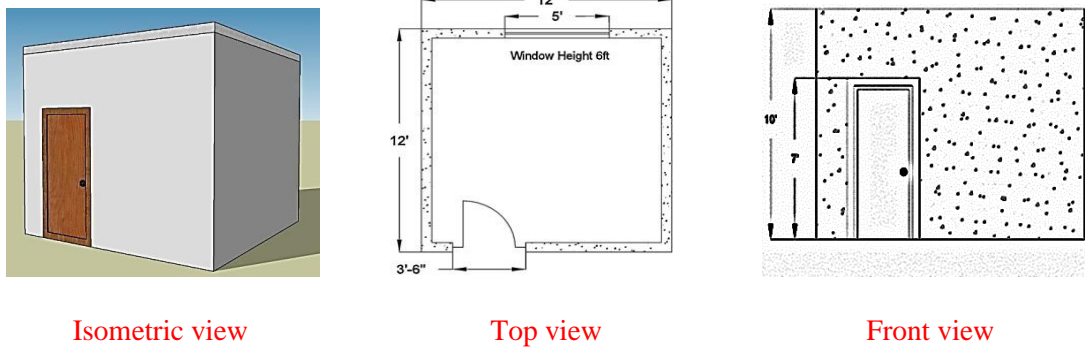


Figure 37: Hypothetical room model

The square room has length and width of 12 feet and a height of 10 feet with a door and window placed on the opposite faces. In order to calculate the absorbing capacity of the room, it is assumed that walls and slab is made up of normal concrete and is plastered using bacterial zeolite grout (BZ) having a thickness of 5 mm. It is also assumed that only external side of room is plastered using BZ grout, the interaction of soil is neglected hence foundations are not accounted for in the calculation. Similarly, additional factors such as population density, green lands, social-economic activities like setting up of industry and urbanization are not considered, therefore the calculations only represent ideal conditions which have been summarized in the table below.

Table 14: Summary of room model calculations

Volume of room	11100203 cm ³
Plaster volume	244374.4 cm ³
CO ₂ absorbed/ cm ³ of plaster	0.025 g/ cm ³
CO ₂ absorbed by room model	6110.55 g

4.4 Healing Cycle

4.4.1 Visual Evidence

In order to investigate the performance of optimum formulation against multiple crack healing cycles, the concrete samples that was repaired with BZ was cracked again until noticeable cracks were formed. It was then left into water tank for water curing for 28 days. Visually almost all the cracks were repaired through autonomous healing. Visual evidence of this autonomous crack healing is given below



Figure 38: Autonomous healing of BZ repaired sample in 2nd cracking cycle

To further authenticate this point, crack width measurement analysis was performed using an optical microscope which clearly indicated in the below image that a crack of width 3.3 mm was autonomously healed after 28 days curing.

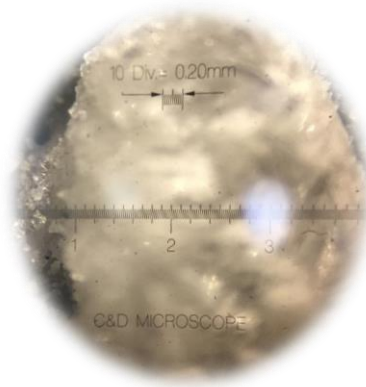


Figure 39: OM image of 2nd healing cycle of BZ repaired concrete

4.5 Cost Comparison

Based on all previous tests results it was concluded that our BZ suspension was founded to be an optimum suspension among all our suspensions. So, cost estimation of BZ was calculated. Quantities to prepare 1 kg BZ were worked out and accordingly the price incurred calculated as shown in tables below from which it can be deduced that BZ is 70 times cost effective solution as compared to epoxy grout.

Table 15: Cost estimation of BZ

B I O – GROUT				
MATERIAL QUANTITES			MARKET RATE	PRICE (PKR)
ITEM	QUANTITY	UNIT		
Cement	.9	kg	500/bag	9
Calcium Lactate	.005	kg	3700/kg	18.5
Nutrient Broth	0.00295	kg	6000/L	17.5
Zeolite	.1	Kg	300/kg	30
			Total	75

Table 16: Cost estimation of epoxy grout

Ratio	3:1
Quantity	0.75 kg
Market Rate	7000/kg
Total	5250 Rs.

CHAPTER 5

CONCLUSIONS

1. BZ, BSAP, BG and BS are suspensions that transferred dead concrete into smart live concrete and re-healing maximum crack width of 3.3 mm
2. BZ being the optimum suspension, recovering compressive and tensile strength up to 96.73% and 92.51% respectively.
3. CO₂ sequestration ability of zeolite immobilized suspension is 32 times the normal concrete and corrosion reduction potential was found to be 1.13% only loss in rebar weight.
4. Prepared bio-suspensions proves to be an effective and cheap (70 times less expensive than commercial epoxy) repairing technique in dead concrete.

RECOMMENDATIONS

Devised Healing suspensions needs to be:

- Analyzed against robustness for multiple crack healing cycles
- Further tested for corrosion and permeability
- Compared with commercially available epoxies
- Monitored against the effects of change temperature on healing efficiency
- CO₂ sequestration must be calculated for BS, BG, BSAP
- Monitored against the effects of humidity on CO₂ sequestration ability of BZ

CONSTRAINTS

1. Due to COVID-19 Pandemic we were not able to carry out many mechanical and forensic tests
2. Difficulty in extracting images from crack width measurement as the instrument is outdated
3. Lack of molds prevent large scale casting; hence the casting regime must be extended so does the testing with difficulty in maintaining testing record
4. Dates of forensic tests were not available at required time.
5. Capacity constraints of temperature-controlled curing tank limits number of samples to be casted for testing

REFERENCES

Wasim Khaliq, Muhammad Basit Ehsan, Crack healing in concrete using various bio influenced self-healing techniques, *Construction and Building Materials* 102 (2016)

Jonkers, H.. (2011). "Bacteria-based self-healing concrete." *Heron*. 56.

Bhaskar, Sini et al. "Effect of self-healing on strength and durability of zeolite-immobilized bacterial cementitious mortar composites." *Cement & Concrete Composites* 82 (2017): 23-33.

Vijay, K., Murmu, M. "Effect of calcium lactate on compressive strength and self-healing of cracks in microbial concrete". *Front. Struct. Civ. Eng.* 13, 515–525 (2019).

M. Guadalupe Sierra-Beltran, H.M. Jonkers, E. Schlangen "Characterization of sustainable bio-based mortar for concrete repair". *Construction and Building Materials* 67 (2014) 344–352

Wiktor, VAC ; Jonkers, HM. "Protection of aged concrete structures: application of bio-based impregnation system. Proceedings of the 1st international conference on ageing of materials and structures," AMS'14. editor K van Breugel ; EAB Koeders. Delft : Delft University of Technology, 2014. pp. 295-301

Henk M. Jonkers, "Toward Bio-based geo- & Civil Engineering for a Sustainable Society" *Procedia Engineering*, Volume 171, 2017, Pages 168-175, ISSN 1877-7058,

Alshalif, Abdullah & Irwan, J.M. & Othman, Norzila & Zamer, Megat & Anneza, L.H.. (2017). "Carbon Dioxide (CO₂) Sequestration In Bio-Concrete, An Overview. MATEC Web of Conferences".

Krishna Lekha R T, and Alester Joseph Vanreyk. "ZEOLITE ADDITION ON CONCRETE SUSTAINABILITY-A REVIEW" *International Journal Of Advance Research And Innovative Ideas In Education* Volume 3 Issue 2 2017 Page 5578-5582

Nassiri, Somayeh. (2011). ESTABLISHING PERMANENT CURL/WARP TEMPERATURE GRADIENT IN JOINTED PLAIN CONCRETE PAVEMENTS. 10.13140/RG.2.2.19167.76964.

Mia HIRATA and Itaru JIMBO "Utilization of Concrete Waste to Capture CO₂

with Zeolite” Proc. Schl. Eng. Tokai Univ., Ser. E41 (2016) 9-13

V. Wiktor, H.M. Jonkers, “Field performance of bacteria-based repair system: Pilot study in a parking garage,” Case Studies in Construction Materials, Volume 2, 2015, Pages 11-17, ISSN 2214-5095,

Kristiawan, Stefanus. (2016). Comparison of shrinkage related properties of various patch repair materials. IOP Conference Series: Materials Science and Engineering. 176. 10.1088/1757-899X/176/1/012017.

Manoj Kumar. C and Dr. Mageswari. M. “RECOVERY OF MECHANICAL PROPERTIES OF SELF HEALING CONCRETE USING SUPER ABSORBENT POLYMER (SAP)” International Journal of Civil Engineering and Technology (IJCIET) Volume 10, Issue 02, February 2019, pp. 202-210,

Ghosh, P., Mandal, S., Chattopadhyay, B.D., and Pal, S., (2005), “Use of microorganism to improve the strength of cement mortar”

Self-Healing Materials, 2010, Martin D. Hager , Peter Greil , Christoph Leyens , Sybrand van der Zwaag , Ulrich S. Schubert

Van Tittelboom, K., De Belie, N., De Muynck, W., and Verstraete, W., (2010), “Use of bacteria to repair cracks in concrete”

Li, V.C., and Yang, E.H., (2007), “Self-healing materials: an alternative approach to 20 centuries of material science

Hirozo Mihashi¹ and Tomoya Nishiwaki, 2012, Development of engineered self-healing and self-repairing concrete, Journal of Advanced Concrete Technology

S.K. Ramachandran, V. Ramakrishnan, S.S. Bang, Remediation of concrete using microorganisms, ACI Mater. J. 98 (1) (2001)

Hammes, F. And Verstraete, W., (2002), “Key roles of pH and calcium metabolism in microbial carbonate precipitation”

Mr.Mengal G.A. and Mr. Shirsath H.A. et al “Co₂ Absorbing Concrete Roads” 6th International Conference on Recent Trends in Engineering & Technology (ICRTET - 2018)

De Muynck, W., Cox, K., Belie, N.D., and Verstraete, W., (2008a), “Bacterial carbonate precipitation as an alternative surface treatment for concrete”

Gaëtan Rimmelé, Véronique Barlet-Gouédard (2010) Accelerated degradation method for cement under CO₂-rich environment: The LIFTCO₂ procedure (leaching induced by forced transport in CO₂ fluids)

H.S. Wong, A.M. Pappas, R.W. Zimmerman, N.R. Buenfeld (2011), Effect of entrained air voids on the microstructure and mass transport properties of concrete

Sormeh Kashef-Haghighi, Yixin Shao, Subhasis Ghoshal (2014), Mathematical modeling of CO₂ uptake by concrete during accelerated carbonation curing

Yves F. Houst I and Folker H. Wittmann (1994), Influence of porosity and water content on the diffusivity of CO₂ and O₂ through hydrated cement paste

Hartt WL, Lee SK, Costa E (1998). Condition assessment and deterioration rate for chloride contaminated reinforced concrete structures

Amir Poursaee (2016), Corrosion of steel in concrete structures

Ahmad, S. (2018), Innovative mix design of cementitious materials for enhancing strength and ductility

Sierra-Beltran, M.G., Jonkers, H.M., and Schlangen, E., (2014), “Characterization of sustainable bio-based mortar for concrete repair”

Palin, D., Wiktor, V., and Jonkers, H.M., (2014), “Towards cost efficient bacteria based self-healing marine concrete”

Achal, V., Mukherjee, A. And Reddy, M.S., (2011), “Microbial concrete: A way to enhance the durability of concrete buildings”

Guadalupe Sierra-Beltran, M., Jonkers, H.M., and Schlangen, E., (2014), “Characterization of sustainable bio-based mortar for concrete repair”

Warda Ashraf (2016), Effects of High Temperature on Carbonated Calcium Silicate Cement (CSC) and Ordinary Portland Cement (OPC) Paste

Forood Torabian Isfahani (2016), Effects of Nanosilica on Compressive Strength and Durability Properties of Concrete with Different Water to Binder Ratio

Broomfield JP (1997). Corrosion of steel in concrete: understanding, investigation and repair.

Bentur A, Diamond S, Berke NS (1997). Steel corrosion in concrete: fundamentals and civil engineering practice

Y. Zhou, B. Gencturk, K. Willam, A. Attar (2015). Carbonation-induced and chloride induced corrosion in reinforced concrete structures

M. Moreno, W. Morris, M.G. Alvarez, G.S. Duffo (2004). Corrosion of reinforcing steel in simulated concrete pore solutions - Effect of carbonation and chloride content

Bertolini L, Elsener B, Pedferri P, Polder R (2003). Corrosion of steel in concrete: prevention, diagnosis, and repair